Quantum simulations of gauge theories with ultracold atoms: Local gauge invariance from angular-momentum conservation

Erez Zohar,[1] J. Ignacio Cirac,[2] and Benni Reznik[1]

[1]*School of Physics and Astronomy, Raymond and Beverly Sackler Faculty of Exact Sciences, Tel Aviv University, Tel Aviv 69978, Israel*

[2]*Max-Planck-Institut für Quantenoptik, Hans-Kopfermann-Straße 1, 85748 Garching, Germany*

(Received 4 June 2013; published 27 August 2013)

Quantum simulations of high-energy physics, and especially of gauge theories, is an emerging and exciting direction in quantum simulations. However, simulations of such theories, compared to simulations of condensed matter physics, must satisfy extra restrictions, such as local gauge invariance and relativistic structure. In this paper we discuss these special requirements, and present a method for quantum simulation of lattice gauge theories using ultracold atoms. This method allows us to include local gauge invariance as a *fundamental* symmetry of the atomic Hamiltonian, arising from natural atomic interactions and conservation laws (and not as a property of a low-energy sector). This allows us to implement elementary gauge invariant interactions for three lattice gauge theories: U(1) (compact QED), $\mathbb{Z}_N$ and SU(N) (Yang-Mills), which can be used to build quantum simulators in $1+1$ dimensions. We also present a loop method, which uses the elementary interactions as building blocks in the effective construction of quantum simulations for $d+1$ dimensional lattice gauge theories ($d>1$), but unlike in previous proposals, here gauge invariance and Gauss's law are natural symmetries, which do not have to be imposed as a constraint. We discuss in detail the quantum simulation of $2+1$ dimensional compact QED and provide a numerical proof of principle. The simplicity of the already gauge-invariant elementary interactions of this model suggests it may be useful for future experimental realizations.

DOI: 10.1103/PhysRevA.88.023617 PACS number(s): 67.85.Hj, 11.15.Ha

I. INTRODUCTION

The concept of quantum simulations goes back to the 1980s, when Feynman suggested the possibility to simulate quantum mechanics using quantum computers [1]. Over the recent decades, the extraordinary progress both in theory and experiments, has enabled an unprecedented control in systems such as cold atoms [2,3] or trapped ions [4]. This control allows us nowadays to use them to simulate other quantum systems in an analog way, in the spirit of Feynman's visionary ideas. This has opened up a path to observe and understand many physical phenomena, which are, at least currently, unreachable in the context of analytic calculations or experimental measurements of the original systems [5].

Of specific interest are quantum simulations of many-body quantum models that appear in condensed matter physics. Some of those models are difficult to handle even with the most advanced numerical techniques, and thus quantum simulation appears as an important tool to investigate them. These models include, for example, Hubbard models, Heisenberg-like models in different lattice geometries. Atomic systems provide us with a natural playground to simulate those models, since once they are loaded in optical lattices, they are basically described in terms of simple Hubbard models whose properties can be tuned with external fields. During the last years, many quantum simulations of such models have been proposed, different techniques have been developed, and some of them have even been realized experimentally.

Gauge theories constitute the fundamental building blocks of the standard model of high-energy physics (HEP). They are built up out of fermionic and bosonic particles (or fields), which represent matter and the force carriers, respectively. As a many-body quantum system, they are extremely rich in intriguing phenomena, and in some limits are very hard to study, even with the most advanced numerical techniques. Thus, a natural question is whether one could use the existing quantum simulators based on atoms in order to observe such phenomena, as well as to investigate regimes where standard techniques do not work. Unlike with condensed matter problems, however, the simulation of HEP models does not appear in a natural way in such atomic systems. In particular, they require: (a) inclusion of both fermions and bosons; (b) interactions preserving local gauge invariance, which results in Gauss's law, as well as (c) Lorentz invariance (at least in the proper continuum limit).

In recent years, several works have proposed to use cold atoms in optical lattices to simulate HEP theories [6–19]. Most of them propose to use optical lattices to enforce condition (c), and perturbation theory such that the desired interacting terms appear in the low-energy sector. In some cases, this may lead to undesirable effects, since the gauge invariance is not exact, or since one has to go to high-order perturbation theory, which leads to very weak effective interactions and strong constraints.

In this paper, building on our early work on quantum simulation of HEP models [10,13,15,17,20], we introduce techniques in order to implement the conditions (a)–(c) above in an optimal manner. First, we propose to use several internal states of the fermionic and bosonic atoms such that the gauge invariance of the resulting HEP model is a direct consequence of the conservation of angular momentum in the original atomic scattering processes, and not a property of the low-energy sector after perturbation theory. Second, since the original Hamiltonian is already gauge invariant, Gauss's law does not have to be enforced: given that (in operator form) it commutes with the Hamiltonian, one just has to initialize the atoms in a state that satisfies it and then the dynamics will always occur in the subspace fulfilling that law.

 ©2013 American Physical Society

Thus, one could start out with the parameters corresponding to a regime where the ground state is well defined, and then turn adiabatically the physical parameters in order to explore other regimes. Third, we propose to engineer the lattice system such that the traps for the bosonic atoms lie between the traps for the fermionic ones. In this way, fermionic hopping is mediated by a collision with the bosonic atoms, giving rise to the matter–gauge-field interactions with the largest possible coefficient, since the overlap integral responsible for this term is maximal. Fourth, we provide a method (the loop method) to construct the plaquette interactions that give rise to the dynamics of the gauge field (in the case of $2+1$ dimensions). As in previous suggestions, we use perturbation theory in order to obtain the effective terms in fourth order. However, we show that lower-order terms in the perturbation series only renormalize our theory, so that we obtain the desired plaquette terms under the conditions that are equivalent to a second-order perturbation (and not to fourth order). Furthermore, unlike in previous proposals, they are constructed out of already gauge-invariant objects, and thus they do not require the explicit use of the Gauss law.

The paper is organized as follows. In Sec. II we put down the basics required for such quantum simulations: We briefly discuss gauge theories and lattice gauge theories, and deduce the requirements that quantum simulations of such systems must fulfill; we discuss simpler high-energy physics models, which already show the interesting physics, but are simpler for quantum simulation, and review previous suggestions for quantum simulations of such systems. In Sec. III we describe the simulating system, the general structure of the optical lattice and atomic Hamiltonian needed for such simulations, and then, in Sec. IV, we show how to get, in the fundamental Hamiltonian (without perturbation theory), the gauge-invariant elementary interactions on links for several gauge theories U(1), $\mathbb{Z}_N$, and SU(N). Then, in Sec. V, we utilize these elementary interactions to build quantum simulations of $1+1$ dimensional models, U(1) (a full nonperturbative simulation of the $1+1$ dimensional Schwinger model) and SU(N). In Sec. VI we introduce the loop method and show how to use the gauge-invariant nonperturbative elementary interactions to construct effectively plaquette interactions, required for the simulation of models in more than $1+1$ dimensions, for these three gauge theories, and in Sec. VII we show how to use them and construct quantum simulators for $2+1$ dimensional lattice gauge theories [U(1), $\mathbb{Z}_N$, and SU(N)]. The paper also contains an appendix, briefly expanding on some properties of the gauge theories whose quantum simulations are discussed.

II. QUANTUM SIMULATION OF HIGH-ENERGY PHYSICS

A. Basics of high-energy physics

The standard model of high-energy physics (HEP) is a quantum field theory (QFT), in which the elementary particles can be divided into two separate groups. Matter particles (quarks and leptons) are fermions, represented by Dirac fields, while the force mediators, which are responsible to the interactions among matter particles, are gauge bosons. Being a gauge boson, the gauge field must satisfy a special symmetry, which is local gauge invariance. This symmetry may be either manifest or broken, but it is the nature of this symmetry that is responsible to the very special coupling between matter and gauge fields. Each gauge theory is based on a gauge group, whose elements are fundamental objects of the theory, forming the group space in which the gauge transformations apply: these transformations do not correspond to changes in any physical observable, and thus they form a symmetry. The gauge groups may be either continuous or discrete, Abelian, and non-Abelian.

Both in Abelian and non-Abelian theories the gauge fields are massless[1]. However, in Abelian theories the gauge fields are chargeless, while in non-Abelian theories they carry charge. Quantum electrodynamics (QED), for example, is an Abelian [U(1)] gauge theory, whose charge is just the ordinary electric charge, and its gauge bosons, the photons, carry no charge. Quantum chromodynamics (QCD), describing the strong interactions, is a non-Abelian [SU(3)] gauge theory, whose charge is the color charge, carried by the quarks but also by the gauge bosons—gluons—due to the non-Abelian nature of the theory. Abelian theories yield linear equations of motion (Maxwell's equations for QED), since the chargeless gauge bosons do not interact among themselves. In non-Abelian gauge theories, there are such self-interactions, due to the non-Abelian charge carried by the gauge bosons, and this results in nonlinear equations of motion: the fundamental theory is described by the Yang-Mills equations for an SU(N) gauge theory [21]. Furthermore, non-Abelian theories are responsible for long-range forces, manifested, for example, by the electromagnetic Coulomb law. However, non-Abelian theories manifest the effect of confinement, which binds matter particles together, such as quark confinement in QCD, which is responsible for the hadronic spectrum and forbids the existence of isolated free quarks [22,23]. This nonperturbative phenomenon has been addressed over the recent decades in a variety of methods, including lattice gauge theories (LGT), where the space time is discretized, enabling a numerical Monte Carlo simulation [22,24–26]. However, such a classical simulation, although very useful for many things, finding the hadronic spectrum, for example, still faces problems such as the sign problem [27], which makes it hard to approach the limit of many fermions (a finite chemical potential), and thus probing some exotic phases of gauge theories (for example, color superconductivity in QCD), which are inaccessible using these methods [28–30]. Other than that, quantum simulations enables also the simulation of dynamics, which is hard to simulate classically.

Another important feature of HEP is being a relativistic theory, i.e., satisfying Lorentz invariance. This is of great significance, as the interactions of elementary particles involve the regime of small distances and, of course, high energies, which requires a relativistic treatment, which is mostly avoidable in the case of condensed matter physics. While this symmetry must be exactly met in the continuum limit, it cannot hold in a discretized space time as in LGTs. However,

[1]In this work we disregard the Higgs mechanism, which breaks the gauge symmetry and gives masses to the gauge fields, and also introduces a *scalar* (bosonic) matter field.

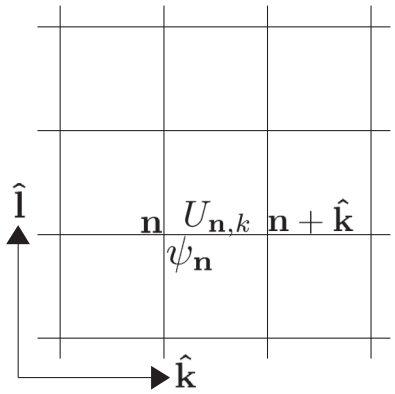

FIG. 1. A part of the spatial lattice, in the $\hat{\mathbf{k}}$-$\hat{\mathbf{l}}$ plane. The labeling of the vertices is shown. The links are labeled by their source vertex and their direction. For example, the link connecting between the vertices $\mathbf{n}$ and $\mathbf{n}+\hat{\mathbf{k}}$ is labeled as $\mathbf{n},k$. A spinor $\psi_{\mathbf{n}}$ is defined on each vertex $\mathbf{n}$, and a group element $U_{\mathbf{n},k}$ is defined on each link $\mathbf{n},k$.

these theories still must include the proper remnants of Lorentz invariance, such that their continuum limit would be exactly relativistic.

B. Basic ingredients of a lattice gauge theory

In lattice gauge theories, one can either discretize the entire (Euclidean) space time, or only the spatial directions. As we are interested in a Hamiltonian model, we shall use the latter latticization, introduced by Kogut and Susskind [24–26].

In Hamiltonian LGTs, the fermionic (spinor) matter degrees of freedom, $\psi_{\mathbf{n}}$ reside on the vertices $\mathbf{n}\in\mathbb{Z}^d$ of a d-dimensional spatial lattice[2] (see Fig. 1). These spinors may carry, generally, other indices, corresponding to possible physical quantum numbers of the matter fields, such as spin or flavor (which we avoid here) and also group space indices, which we denote here by lowercase roman letters, a,b, etc. And thus, generally

$$\psi_{\mathbf{n}}=(\psi_{\mathbf{n},a})=\begin{pmatrix}\psi_{\mathbf{n},1}\\ \psi_{\mathbf{n},2}\\ \dots\end{pmatrix} \tag{1}$$

the dimension of the spinor depends on the representation r of the gauge group used for it. Such fields may have local (mass) terms in the Hamiltonian, with the most general form

$$H_M=\sum_{\mathbf{n}}M_{\mathbf{n}}\psi^{\dagger}_{\mathbf{n}}\psi_{\mathbf{n}}, \tag{2}$$

where summation on the group indices is implicitly included, of course ($\psi^{\dagger}_{\mathbf{n}}\psi_{\mathbf{n}}=\sum_a\psi^{\dagger}_{\mathbf{n},a}\psi_{\mathbf{n},a}$). These terms are gauge invariant, as the group indices are fully contracted. Another way to see the gauge invariance is to consider the explicit local gauge transformation on the matter fields,

$$\psi_{\mathbf{n}}\to V^r_{\mathbf{n}}\psi_{\mathbf{n}}=\sum_b\left(V^r_{\mathbf{n}}\right)_{ab}\psi_{\mathbf{n}b}, \tag{3}$$

where $V_{\mathbf{n}}$ is an element of the group, represented by the unitary matrix $V^r_{\mathbf{n}}$ in the same representation of $\psi_{\mathbf{n}}$, defined locally for each vertex $\mathbf{n}$, and see that it leaves these terms invariant.

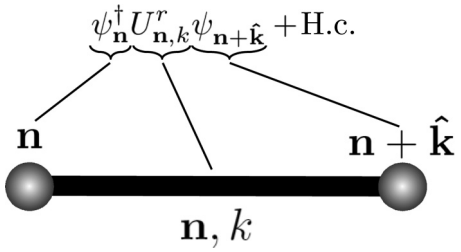

FIG. 2. The elementary interactions: the interaction between the neighboring vertices $\mathbf{n}$ and $\mathbf{n}+\hat{\mathbf{k}}$ involves the gauge field on the link $\mathbf{n},k$ connecting them, thus the gauge bosons are interaction mediators. As discussed in Sec. IV, this is the natural type of interaction in our simulation scheme, included in the fundamental atomic Hamiltonian.

The interactions among the matter fields must include the gauge fields as well, being the force mediators. As such, the most reasonable place for the gauge degrees of freedom is on the lattice's links. Thus, on each link of the lattice, emanating from the vertex $\mathbf{n}$ in direction k, define a group element $U_{\mathbf{n},k}$ (see Fig. 1). These elements can be represented by any representation r of the group. In general, $U_{\mathbf{n},k}$ are matrices of operators, defined on the link's local Hilbert space. This matrix space is called group space, and the matrix indices, a,b, etc., are referred to as group indices. Explicit examples of such $U_{\mathbf{n},k}$ matrices of operators will be shortly presented.

The interaction between neighboring vertices is mediated using the link connecting them, in the form of elementary interactions (see Fig. 2)

$$\begin{aligned}H_{\text{int}}&=\epsilon\sum_{\mathbf{n},k}\left(\psi^{\dagger}_{\mathbf{n}}U^r_{\mathbf{n},k}\psi_{\mathbf{n}+\hat{\mathbf{k}}}+\text{H.c.}\right)\\&=\epsilon\sum_{\mathbf{n},k}\sum_{a,b}\left(\psi^{\dagger}_{\mathbf{n},a}\left(U^r_{\mathbf{n},k}\right)_{ab}\psi_{\mathbf{n}+\hat{\mathbf{k}},b}+\text{H.c.}\right),\end{aligned} \tag{4}$$

where U^r is the matrix representation of U in r, the spinors's representation. Once again, these terms are gauge invariant as all the group's indices are contracted. One can also deduce, from the transformation law of the spinors (3) and the gauge invariance demand, the transformation law of U,

$$\begin{aligned}U^r_{\mathbf{n},k}&\to V^r_{\mathbf{n}}U^r_{\mathbf{n},k}V^{\dagger r}_{\mathbf{n}+\hat{\mathbf{k}}}\\ \left(U^r_{\mathbf{n},k}\right)_{ab}&\to\sum_{c,d}\left(V^r_{\mathbf{n}}\right)_{ac}\left(U^r_{\mathbf{n},k}\right)_{cd}\left(V^{\dagger r}_{\mathbf{n}+\hat{\mathbf{k}}}\right)_{db}.\end{aligned} \tag{5}$$

Finally, one shall introduce the pure-gauge terms as well. One type of pure-gauge term which is gauge invariant, is of the form

$$H_E=\frac{g^2}{2}\sum_{\mathbf{n},k,a}(E_{\mathbf{n},k})_a(E_{\mathbf{n},k})_a, \tag{6}$$

where $(E_{\mathbf{n},k})_a$ are the generators of the group's algebra, for example, an angular momentum algebra for SU(2), consisting

[2]Lattice fermions are a complicated subject of its own, due to the problem of fermion doubling in the continuum limit. This problem can be resolved in several ways, but we shall not consider it here as it is irrelevant for our discussion.

of the angular momentum operators as generators. This term is just a sum of Casimir operators [which commute with all the generators, such as the total angular momentum operator for SU(2)], and it is interpreted as the electric energy. In general, one can define left (L_a) and right (R_a) generators on each link, constrained to give the same Casimir operator $\sum_a L_a L_a = \sum_a R_a R_a \equiv \sum_a E_a E_a$.

These electric field also construct the generators of local gauge transformations,

$$(G_{\mathbf{n}})_a = \mathrm{div}_{\mathbf{n}} E_a - Q_{\mathbf{n}}, \tag{7}$$

where $\mathrm{div}_{\mathbf{n}} E_a$ is the discrete divergence of the group,

$$\mathrm{div}_{\mathbf{n}} E_a = \sum_k [(L_{\mathbf{n},k})_a - (R_{\mathbf{n}-\hat{\mathbf{k}},k})_a] \tag{8}$$

and $Q_{\mathbf{n}}$ is the local charge (either dynamic or static). These generators are constants of motion—the physical states are the gauge-invariant ones, satisfying, for each vertex $\mathbf{n}$, the Gauss's law

$$(G_{\mathbf{n}})_a |\mathrm{phys}\rangle = 0. \tag{9}$$

Another type of gauge-invariant Hamiltonian term is the trace of group elements along a closed path. The shortest such paths are plaquettes, and they form the magnetic energy part (see Fig. 3),

$$H_B = -\frac{1}{g^2} \sum_{\text{plaquettes}} [\mathrm{Tr}(U_1 U_2 U_3^\dagger U_4^\dagger) + \mathrm{H.c.}], \tag{10}$$

where the 1,2,3,4 links are oriented along a plaquette (see Fig. 3). The trace is on group (matrix) indices.

Usually one includes in the Hamiltonian all such terms, where all the objects (group elements and spinors) are chosen to be in the fundamental representation. This will also be our choice throughout the paper.

Next, let us give some explicit examples of three gauge theories we use and simulate in this paper. We shall describe the structure and Hilbert space of these theories, whereas further details can be found in the Appendix.

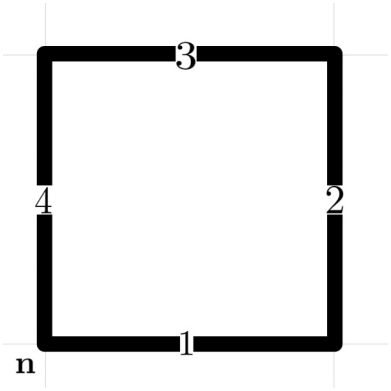

FIG. 3. The plaquette interactions: the gauge-gauge interactions. The labeling of the links around the plaquette is according to Eq. (10). As discussed in Sec. VI, these interactions are obtained effectively in our simulation scheme.

1. Compact QED

As a basic example, we discuss compact QED (cQED). This is an Abelian gauge theory, with the gauge group U(1), whose continuum limit is regular QED. However, unlike continuous QED, this theory manifests confinement of charges: at all values of the coupling constant g for $1+1$ and $2+1$ dimensions, and in the strong coupling regime for $3+1$ dimensions [23,25,31,32]. The compactness of the theory is essential for the existence of a confining phase [33].

In this theory, the $U_{\mathbf{n},k}$ operators defined on the links are pure phases: $U_{\mathbf{n},k} = e^{i\phi_{\mathbf{n},k}}$. The conjugate electric field $E_{\mathbf{n},k}$ is merely an angular momentum operator, taking integer values from $-\infty$ to ∞. Thus, on each link $U_{\mathbf{n},k}$ the Hilbert space is the one of a quantum rotor, with canonical variables satisfying

$$[E_{\mathbf{n},k}, \phi_{\mathbf{m},l}] = -i\delta_{\mathbf{nm}}\delta_{kl}. \tag{11}$$

This makes the U operators ladder operators of angular momentum, or, in other words, of electric flux

$$U_{\mathbf{n},k}|m\rangle = e^{i\phi_{\mathbf{n},k}}|m\rangle = |m+1\rangle. \tag{12}$$

Note that as this group is Abelian, there is no need to use different left and right generators. As there is only one generator, Gauss's law (9) simplifies to

$$(G_{\mathbf{n}})|\mathrm{phys}\rangle = 0, \tag{13}$$

where $G_{\mathbf{n}} = \sum_k (E_{\mathbf{n},k} - E_{\mathbf{n}-\hat{\mathbf{k}},k})$.

Using these operators, we can deduce from the general Hamiltonians (6), (10) the Abelian version of the Kogut-Susskind Hamiltonian,

$$H_{\mathrm{KS}} = H_E + H_B = \frac{g^2}{2}\sum_{\mathbf{n},k} E_{\mathbf{n},k}^2 - \frac{1}{g^2}\sum_{\mathbf{n}} \cos(\phi_{\mathbf{n},1} + \phi_{\mathbf{n}+\hat{\mathbf{1}},2} - \phi_{\mathbf{n}+\hat{\mathbf{2}},1} - \phi_{\mathbf{n},2}). \tag{14}$$

In the continuum limit, H_E is identified with the electric energy and H_B with the magnetic one [as the cosine's argument is the curl of the vector potential: $\cos(\phi_{\mathbf{n},1} + \phi_{\mathbf{n}+\hat{\mathbf{1}},2} - \phi_{\mathbf{n}+\hat{\mathbf{2}},1} - \phi_{\mathbf{n},2}) \to 1 - \frac{B^2}{2}$]. As for H_{int}, using staggered fermions [34] (see the Appendix), we only have one spinor at each vertex, and in this case (4) is simplified to

$$H_{\mathrm{int}} = \epsilon \sum_{\mathbf{n},k} (\psi_{\mathbf{n}}^\dagger e^{i\phi_{\mathbf{n},k}} \psi_{\mathbf{n}+\hat{\mathbf{k}}} + \psi_{\mathbf{n}+\hat{\mathbf{k}}}^\dagger e^{-i\phi_{\mathbf{n},k}} \psi_{\mathbf{n}}) \tag{15}$$

and thus the basic interaction involves a fermion hopping between neighboring vertices, while raising or lowering, depending on the direction of the hopping fermion, the electric flux on the link connecting them (see Fig. 4). For further details, refer to the Appendix.

2. $\mathbb{Z}_N$ gauge theory

Here we shall review the properties of a Hamiltonian $\mathbb{Z}_N$ gauge theory [35]. We restrict ourselves to the pure-gauge case, as only this is relevant for the purposes of this paper.

First, let us describe the local Hilbert space on every link of the lattice. Define two operators, P, Q, which are unitary

$$P^\dagger P = Q^\dagger Q = 1 \tag{16}$$

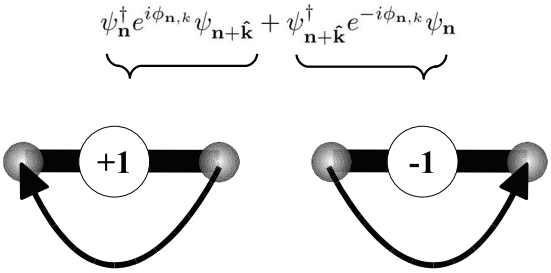

FIG. 4. Illustration, using the U(1), of the directionality of elementary interactions (15). If a fermion hops to the left, the flux in the middle increases. If a fermion hops to the right, the flux in the middle decreases.

and satisfy the $\mathbb{Z}_N$ algebra,

$$P^N = Q^N = 1; \quad P^\dagger Q P = e^{i\delta} Q \tag{17}$$

where $\delta = \frac{2\pi}{N}$.

For example, one can work with the basis of P eigenstates,

$$P|m\rangle = e^{im\delta}|m\rangle \tag{18}$$

with $m \in \{-N/2, \ldots, N/2\}$ (without loss of generality, we assume N is odd; the change for an even N is straightforward) and then Q is a unitary ladder operator,

$$Q|m\rangle = |m-1\rangle \tag{19}$$

with the cyclic property $Q|-N/2\rangle = |N/2\rangle$. Alternatively, one can expand the Hilbert space in terms of Q eigenstates, and then P will be a unitary raising operator (with the cyclic property, again).

Interestingly, one can introduce the Hermitian operators E, A on every link, by

$$P = e^{i\delta E}; \quad Q = e^{iA} \tag{20}$$

and then, for $N \to \infty$, one obtains the cQED Hilbert space, with canonically conjugate E, A.

Let us now combine the entire lattice in order to get the gauge-invariant Hamiltonian. It has the form

$$H = H_E + H_B = -\frac{1}{2}\mu \sum_{\mathbf{n},k} (P_{\mathbf{n},k} + P^\dagger_{\mathbf{n},k}) - \frac{1}{2}\sum_{\mathbf{n}} (Q_{\mathbf{n},1} Q_{\mathbf{n}+\hat{\mathbf{1}},2} Q^\dagger_{\mathbf{n}+\hat{\mathbf{2}},1} Q^\dagger_{\mathbf{n},2} + \text{H.c.}). \tag{21}$$

One can define a static modular charge on the vertex $\mathbf{n}$, by $q_{\mathbf{n}} = e^{-i\delta m}$. Then the Gauss's law means that a gauge-invariant state must satisfy (for every $\mathbf{n}$),

$$G_{\mathbf{n}}|\text{phys}\rangle = q_{\mathbf{n}}|\text{phys}\rangle, \tag{22}$$

where

$$G_{\mathbf{n}} = \prod_{l+} P^\dagger_{l+} \prod_{l-} P_{l-} = e^{-i\delta \text{div}_{\mathbf{n}} E} \tag{23}$$

with l_+ are links starting at $\mathbf{n}$ (positive links), and l_- are ending there (negative links). Since these charges are modular and thus very different than the charges of continuous gauge theories, we shall only consider the pure-gauge case for $\mathbb{Z}_N$ in this paper.

3. *SU(N) gauge theories*

Let us first discuss the links' Hilbert space for a pure-gauge theory. In a representation r, with representation matrices $\{T^r_a\}$, the group elements can be parametrized as

$$U^r_{\mathbf{n},k} = e^{i\sum_a T^r_a \phi^a_{\mathbf{n},k}}; \tag{24}$$

it is a matrix in group space.

Due to the non-Abelian nature of the gauge group, it must have separate left and right generators, $\{L_a\}, \{R_a\}$ respectively, corresponding to left and right non-Abelian electric fields [24,26]: they can be represented as differential operators, canonically conjugate to the group parameters $\{\phi^a_{\mathbf{n},k}\}$. As left and right generators of the group, they obey the following commutation relations with the group elements (within the same link, of course)

$$[L_a, U^r] = T^r_a U^r; \quad [R_a, U^r] = U^r T^r_a \tag{25}$$

and the Lie algebra

$$[L_a, L_b] = -i f_{abc} L_c; \quad [R_a, R_b] = i f_{abc} R_c, \tag{26}$$

where f_{abc} are the group's structure constants[3], and also $[L_a, R_b] = 0$. Physically, the difference between the left and right generators of a link may be interpreted as the color charge of it. The left and right generators can be obtained from each other using the group element on the link in the adjoint representation.

From the local gauge transformation (5), one can conclude that the generators of local groups transformation are (7), where in the pure-gauge case $Q_{\mathbf{n}}$ are C numbers.

From now on, we shall focus mostly on SU(2), the simplest continuous non-Abelian group. There [24], $r = j$ (total angular momentum quantum number), $f_{abc} = \epsilon_{abc}$. The local Hilbert space is characterized by three integer quantum numbers, j, m, m', which are eigenvalues of the Casimir operators and the z components of left and right angular momentum

$$\sum_a E_a E_a |jmm'\rangle = \sum_a L_a L_a |jmm'\rangle = \sum_a R_a R_a |jmm'\rangle = j(j+1)|jmm'\rangle \tag{27}$$

$$L_z|jmm'\rangle = m|jmm'\rangle; \quad R_z|jmm'\rangle = m'|jmm'\rangle. \tag{28}$$

The link Hilbert space may be interpreted as the one of a rigid rotator. The generators in the two edges of a link may then be interpreted as generators of rotations in the body/space systems [24]. The link's structure, in terms of operators and Young tableaux, is presented in Fig. 5.

What shall be the Hamiltonian of such a theory? If we require it to be gauge invariant, it may contain only gauge-invariant terms. Such terms can be constructed out of the generators, and since they must be contracted we get the

[3]One should note that one can have $[L_a, L_b] = i f_{abc} L_c$. That results in a redefinition of the left generators, resulting in sign changes in its commutator in (25), gauge generators (7) and Gauss's law, etc.

FIG. 5. The link's operators. Left and right generators $\{L_a\},\{R_a\}$, and the group element. The generators transform in the adjoint representation ($j = 1$), as symbolized by the Young tableaux, and are related to each other by the rotation matrix $U^1(\mathbf{n},k)$ (which is in the adjoint representation as well).

Casimir operators $L_aL_a = R_aR_a$. They construct the local part of the Hamiltonian, called the electric part, H_E (6). Other possibilities are closed loops: the most local ones are the traces of group elements directed around a single plaquette, forming the magnetic part. We choose them to be in the fundamental representation ($T_a = \frac{1}{2}\sigma_a$, where σ_a are Pauli matrices) to get H_B (10), and finally obtain the SU(2) version of the Kogut-Susskind Hamiltonian [24], $H = H_E + H_B$.

C. Basic requirements for a HEP quantum simulation

As can be understood from above, quantum simulation of HEP may be of great interest, and also significance, as it may help in avoiding problems of classical simulation, such as the sign problem. However, one should note it requires much more complex ingredients than quantum simulation of condensed matter systems: Quantum simulation of HEP models must

(i) Include both fermions and bosons, if one wishes to simulate both matter and gauge fields. This requires, for a cold-atom simulations, the use of many different atomic species.

(ii) Respect local gauge invariance, in order to have the correct symmetry, which is responsible to the interactions and the interesting special features of the theories.

(iii) Be relativistic. This can be reduced, if a lattice gauge theory is simulated, demanding that the continuum limit will still be relativistic.

If one chooses to work on the lattice, as we do, the local gauge invariance problem transforms to the challenge of obtaining two types of interactions. First, the link gauge-matter interaction (4), which couples the matter and gauge field degrees of freedom in a very special way; Our basic idea is to get these interactions fundamentally in the atomic Hamiltonian; they will be derived directly from the conservation of hyperfine angular momentum $\mathbf{F}$ in atomic collisions.

The second type of interactions are the plaquette interactions (10), which are, essentially, four-body interactions—not a fundamental part of the atomic Hamiltonian. However, as we show, these terms can be obtained effectively from the link terms, using perturbation theory [36,37]. Although they are obtained effectively, gauge invariance is still fundamental, as the building blocks, elementary interactions, already fulfill the gauge symmetry.

D. HEP toy models

Simulations of gauge theories, which must satisfy all the three requirements presented above, are challenging. However, when simulating HEP phenomena, one would not necessarily need, in first stage, to simulate the entire standard model, or even quantum chromodynamics. Several simpler models are available for observing the important phenomena and phases of the complicated theories. For example, working on the lattice, compact QED is suitable for observing confinement (see Appendix A1): although everyday continuous QED manifests the opposite behavior of a Coulomb phase, the compact lattice theory contains a confining phase in the strong coupling limit of the $3+1$ dimensional theory, and confines for any value of the coupling constant in the $1+1$ and $2+1$ dimensional theories [23,25,31,32]. Thus, for the observation of confinement in a pure-gauge theory, simulation of $2+1$ cQED is enough (the $1+1$ dimensional model is trivial). If one wishes to introduce dynamic charges, even the $1+1$ dimensional case is interesting, for example, one could simulate the lattice version of the Schwinger model [38].

As for non-Abelian theories, full-fledged QCD with an SU(3) gauge symmetry is not essentially required as well, for the first step. A lot of theoretical, both qualitative and quantitative insight has been gained on QCD using the $1+1$-dimensional version of the theory, QCD_2, or more generally, SU(N) in $1+1$ dimensions [39–45]. On the other hand, some phenomena, such as confinement, may be observed also using a smaller gauge group, SU(2). Thus, for simulations of non-Abelian gauge theories, SU(2) on the lattice [46], even in $1+1$ dimensions, is enough.

E. Summary of previous works

Several suggestions have been made for simulations of quantum field theories, which do not include gauge fields. These include the observation of vacuum entanglement of a scalar field using trapped ions [47], and the simulation of interacting scalar and fermionic fields: Thirring and Gross-Neveu models using cold atoms [6] (the latter could also be interpreted as a $1+1$ simulation of fermions coupled to a gauge field). These two models correspond to simulation of fields in the continuum, respecting the appropriate relativistic and causal structure. Quantum computation of scattering amplitudes for scalar field theories was introduced in [48,49]. Simulations of fermionic lattice QFTs have been proposed as well, where the fermions were either free or in external nondynamical gauge fields. These include Axions and Wilson fermions [7], Dirac fermions in curved space time [8], and general quantum simulators of QFTs and topological insulators [11].

As for Abelian pure-gauge theories, simulation of $2+1$ dimensional ($2+1$-d) cQED, with the possibility to observe confinement, first using Bose-Einstein condensates (BECs) of ultracold atoms in optical lattices [10] and then with single atoms in optical lattices [13] have been suggested, where the first is of the Abelian Kogut-Susskind Hamiltonian [24] and the latter of a truncated spin-gauge theory.

The inclusion of dynamical matter in such theories of great interest as well. This was done either for the link model [50–53]—a $1+1$-d simulation of the lattice Schwinger model [14]—or as a generalization of the previous pure-gauge simulations in $2+1$ dimensions, to include dynamical fermions [15]. The latter also suggested a way to realize the gedanken experiment proposed in Ref. [20] of measuring Wilson-Loop's area law.

All these Abelian proposals fulfilled the relativity requirement through the use of the lattice. The models that included simulations fulfilled the first requirement by either including

both fermions and bosons, or enabling the simulation of both types of particles. The gauge-invariance demand has also been met, however, it has not been done in a direct way: gauge symmetry is not fundamental in these models, but rather appears as a low-energy symmetry, manifested in the dynamics of an effective Hamiltonian, obtained using a Gauss's law constraint required to introduce gauge invariance: this is since the four-body plaquette interactions are not fundamental for optical lattices. In Ref. [54], the possibility of interpreting the breaking of the Gauss's law constraint as the emergence of Higgs fields is discussed, in the context of the simulation proposed in Ref. [10].

Simulations of other Abelian lattice gauge theories are presented in Refs. [16,55]. One should also note the continuum QED simulation proposed in Ref. [9] (which does not manifest confinement as it is not compact [33]).

Some proposals for the simulations of non-Abelian models have already been proposed as well, either utilizing prepotentials [56], using ultracold atoms in optical lattices [17], or utilizing Rishons in the link model [18]. In both methods a constraint is used in order to obtain the desired interactions. A digital simulation of an SU(2) gauge magnet [51,57] has also been suggested [19]. In Ref. [18], as in non-Abelian link models, the original symmetry is larger and one has to break it in order to obtain the right symmetry group; in Ref. [17], the SU(2) gauge symmetry is fundamental and is manifested already by the basic atomic Hamiltonian, unlike the effective methods of the former Abelian simulations. This is done by exploiting the fundamental angular momentum conservation of the atoms, in a way which will be further explained and utilized for simulating other gauge theories in the next sections of this paper. A realization of discrete gauge theories (such as $\mathbb{Z}_N$) has been discussed using Josephson junctions [58].

F. Present work

We have introduced the requirements from the quantum simulations of a gauge theory. As explained, in the previous proposals for simulations of Abelian theories, gauge invariance was effective, rather than exact. Here we shall describe the way to utilize a fundamental symmetry in systems of ultracold atoms in order to get a gauge symmetry, which is not an effective low-energy symmetry, but rather built into the theory, and thus is more robust.

In the simulating scheme we suggest in this paper, we use fermions as matter and bosons as gauge fields, in vertices and links, respectively, like in the previous proposals. However,

(i) *Local gauge invariance*. We do not impose Gauge invariance using an energy penalty in the Hamiltonian. Instead, we show that by a judicious choice of fermionic and bosonic species (i.e., internal states), the natural atomic scattering interactions give rise to the terms we need with the appropriate gauge symmetries. This is so because the gauge symmetry in the resulting HEP model is equivalent to the angular momentum conservation in the collisions in the atomic model.

(ii) *Elementary interactions on links*. The interaction terms between bosons and fermions are chosen so that they are maximal, and can compete with the real tunneling. This is obtained by using the idea of Fig. 7 (see next section).

(iii) *Plaquette interactions*. In $2+1$ dimensional systems (and more), in order to obtain the dynamical terms of the gauge bosons (plaquette terms), we must use fourth-order perturbation theory, introducing the loop method. This would naively mean that we get very small terms. However, we make sure that the odd orders are canceled (or just renormalize previous terms), so that in reality the conditions are equivalent to a second-order perturbation theory, which are not so small. The plaquette interactions are $O(\epsilon^4)$ [where ϵ is defined in Eq. (4)], but ϵ,ϵ^3 and the other odd orders of ϵ are absent in the perturbative series, and thus the expansion parameter is ϵ^2 and effectively it is a second-order contribution: $O[(\epsilon^2)^2]$.

Resulting from that, we

(i) Propose a $1+1$ dimensional cQED simulation, which should be relatively simple to implement experimentally.

(ii) Extend it to $2+1$ dimensional cQED by adding plaquette terms, and also introduce a $2+1$ dimensional model, $\mathbb{Z}_N$.

(iii) Suggest a method for simulation of SU(N) theories, including a possible extension of the SU(2) model considered in Ref. [17] to $2+1$ dimensions.

III. SIMULATING SYSTEM

Let us consider the atomic ingredients. We would like to build a theory of both fermions and bosons, where the fermions reside on the vertices, and the bosons on the links (see Fig. 6). Thus, let us start with the most general such structure. The vertices $\mathbf{n}$ of a square optical lattice coincide with the minima of fermions, described by the second-quantization operators $\Psi_\alpha(\mathbf{x})$, where α labels the atomic species. Each link of this lattice coincides with a bosonic minimum, in which the bosons $\Phi_\alpha(\mathbf{x})$ may reside. If one assumes that the single-particle energy levels of each minimum are remote enough, only the lowest Bloch bands may be considered, and thus the second-quantized field operators may be expanded in terms of local annihilation operators $c_{\mathbf{n},\alpha}, a_{\mathbf{n},k,\alpha}$ and local Wannier functions $\psi_{\mathbf{n},\alpha}(\mathbf{x}), \phi_{\mathbf{n},k,\alpha}(\mathbf{x})$, for fermions on the vertex

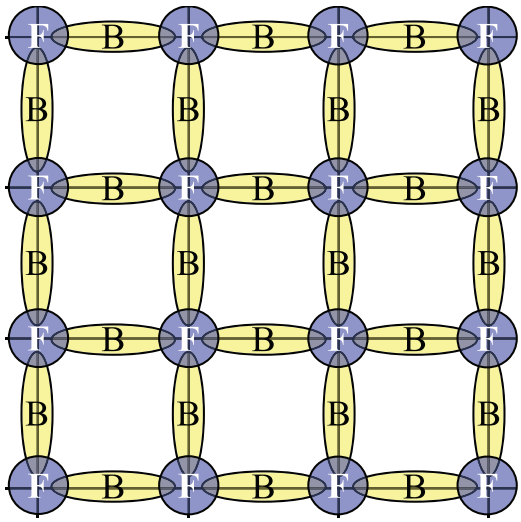

FIG. 6. (Color online) Schematic structure of the optical lattice used for simulations: Bosonic minima on the links (B), and fermionic minima on the vertices (F).

n and bosons on the link emanating from it to the $\hat{\mathbf{k}}$ direction respectively,

$$\Psi_\alpha(\mathbf{x}) = \sum_{\mathbf{n},\alpha} c_{\mathbf{n},\alpha}\psi_{\mathbf{n},\alpha}(\mathbf{x})$$
$$\Phi_\alpha(\mathbf{x}) = \sum_{\mathbf{n},k,\alpha} a_{\mathbf{n},k,\alpha}\phi_{\mathbf{n},k,\alpha}(\mathbf{x}). \tag{29}$$

The most general atomic Hamiltonian contains the following terms:

(i) Single-particle terms

$$H_0 = \sum_\alpha \int d^3\mathbf{x}[\Psi_\alpha^\dagger(\mathbf{x})H_{0,f}\Psi_\alpha(\mathbf{x}) + \Phi_\alpha^\dagger(\mathbf{x})H_{0,b}\Phi_\alpha(\mathbf{x})], \tag{30}$$

where H_0,f, H_0,b are the single-particle Hamiltonians, containing the kinetic energy and the trapping potentials, for the fermions and bosons respectively. Once the expansion (29) is plugged into these terms, and the overlap of Wannier functions is taken into account in the integration, one obtains two types of terms: local terms, linear in the atomic numbers, and nearest-neighbor hopping terms. In order to eliminate the latter for bosons, one should design the bosonic lattice deep enough such that any interactions outside a bosonic minimum would be negligible. In order to avoid fermionic tunneling, one could use different species at neighboring vertices, alternately.

(ii) Scattering terms

$$\begin{aligned} H_{sc} = &\sum_{\alpha,\beta,\gamma,\delta} g^{FF}_{\alpha\beta\gamma\delta}\int d^3\mathbf{x}\Psi_\alpha^\dagger(\mathbf{x})\Psi_\beta^\dagger(\mathbf{x})\Psi_\gamma(\mathbf{x})\Psi_\delta(\mathbf{x}) \\ &+ \sum_{\alpha,\beta,\gamma,\delta} g^{BB}_{\alpha\beta\gamma\delta}\int d^3\mathbf{x}\Phi_\alpha^\dagger(\mathbf{x})\Phi_\beta^\dagger(\mathbf{x})\Phi_\gamma(\mathbf{x})\Phi_\delta(\mathbf{x}) \\ &+ \sum_{\alpha,\beta,\gamma,\delta} g^{BF}_{\alpha\beta\gamma\delta}\int d^3\mathbf{x}\Psi_\alpha^\dagger(\mathbf{x})\Psi_\beta(\mathbf{x})\Phi_\gamma^\dagger(\mathbf{x})\Phi_\delta(\mathbf{x}), \end{aligned} \tag{31}$$

where the scattering coefficients $g^{FF}_{\alpha\beta\gamma\delta}, g^{BB}_{\alpha\beta\gamma\delta}, g^{BF}_{\alpha\beta\gamma\delta}$ are constrained by conservation laws and are fixed for different atoms, but can be controlled and modified using Feshbach resonances (perhaps optical, [59–61], if more than one is required). The first two terms represent the fermion-fermion and boson-boson scattering. Their integration, using (29), yields local scattering terms, within the same minima.

(iii) Rabi (laser) terms

$$\begin{aligned} H_R = &\sum_{\alpha,\beta}\Omega^F_{\alpha\beta}\int d^3\mathbf{x}\Psi_\alpha^\dagger(\mathbf{x})\,\Psi_\beta(\mathbf{x}) \\ &+ \sum_{\alpha,\beta}\Omega^B_{\alpha\beta}\int d^3\mathbf{x}\Phi_\alpha^\dagger(\mathbf{x})\,\Phi_\beta(\mathbf{x}). \end{aligned} \tag{32}$$

Using such terms, one can create manually desired hopping processes, which may be useful in several cases.

In principle one could also consider molecular terms, which dissociate into atoms, giving rise to a term with a bosonic operator and two fermionic ones. This may be useful for simulations in the bulk, but will not be used in the present paper where we concentrate on lattices.

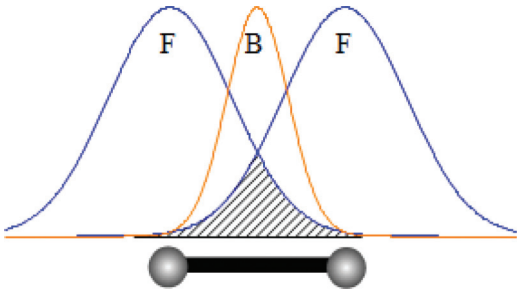

FIG. 7. (Color online) A schematic plot of the overlap of the fermionic Wannier functions (F) of two neighboring vertices and the bosonic Wannier functions (B) on the link. This is because the bosonic overlap is of order 1 and the fermionic tunneling is thus maximal.

IV. ELEMENTARY INTERACTIONS ALONG LINKS

In this section we show how the fermion-gauge boson interaction terms appear in a natural way in the atomic system if one makes a judicious choice of internal states. Since the elementary interactions must come from the scattering of fermions with bosons [Eq. (31)], it must involve an overlap integral between the initial and final bosonic and fermionic states. Given the fact that the fermions must hop, those two states will be located at different positions. In order to make this term as large as possible, one must have the bosonic atoms placed in between the fermionic ones (see Fig. 7). Furthermore, in order to satisfy the gauge symmetry we will choose that the fermions and bosons change the internal states in this process according to the angular momentum conservation.

The key idea is angular momentum conservation: in these atomic scattering processes, the total hyperfine angular momentum $\mathbf{F}_{\text{tot}}$ is conserved. In particular, the z components, m_F, are conserved. One can specifically select the m_F values of the atomic species utilized, in order to generate the required interactions over the link, and eliminate the others. This will result in only gauge-invariant terms, and forms the correspondence between two fundamental symmetries: angular momentum conservation in the atomic, simulating level, is equivalent to gauge invariance in the simulated. Let us first discuss the case of an Abelian H_{int}, as in (15).

A. U(1) elementary interactions

For simulating cQED, we need two fermionic species and two bosonic species[4], arranged in an optical lattice, as in the previous section. Let us first consider a one-dimensional lattice, and thus the links may be labeled only by one index—the vertex from which they emanate—however, the same method may be generalized for more spatial dimensions, as we shall later do.

We start with the bosons. Denote that bosonic species a,b, both having two different values of m_F. As explained before, no interactions take place between bosons of different links. Thus the total number of bosons on each link is a constant of motion; we denote it by N_0, setting it equal all around the lattice, and taking it to be an even number.

[4]As will be later explained, one could use only one fermionic species, and replace the fermions with more bosons.

On each link, a Schwinger algebra [62,63] is constructed from the two bosonic species

$$L_+ = a^\dagger b; \quad L_- = b^\dagger a \tag{33}$$

and

$$L_z = \frac{1}{2}(N_a - N_b); \quad \ell = \frac{1}{2}(N_a + N_b) = \frac{N_0}{2} \tag{34}$$

where L_z is our (truncated) electric field.

Next, we wish to consider the fermions. As we would like to simulate a staggered fermions model ([34,38], see Appendix A2), we only need a single fermion at most on each vertex. However, in order to use angular momentum conservation to ensure gauge invariance, we must use two different fermions, labeled by c and d, arranged such that the c minima occur in even vertices and the d minima in odd vertices. This eliminates the fermionic nearest-neighbor tunneling of H_0. The lattice is designed such that we get from H_0 the mass Hamiltonian

$$H_M = M\sum_n (-1)^n \psi_n^\dagger \psi_n \tag{35}$$

where ψ_n is either c_n or d_n, depending on the parity of the vertex. The Dirac sea state is obtained if initially all the d vertices are filled and the c vertices are empty. Note that if $M > 0$, the fermionic minima do not have to be m_F dependent: if the system is initially prepared in a gauge invariant state, the fermionic tunneling of H_0 is energetically forbidden and thus effectively eliminated and can be disregarded. Moreover, it also assures that two fermions can never occupy a single vertex (even of a different species), and thus the fermion-fermion scattering terms of H_{sc} may be disregarded. The fermions' local charges are defined as $Q_n = \psi_n^\dagger \psi_n - \frac{1}{2}[1-(-1)^n]$. For further details, see Appendix A2.

The gauge-invariant elementary interactions are obtained from the boson-fermion scattering [the third part of H_{sc} (31)]. This is done by utilizing the total m_F in atomic collisions. The hyperfine levels of the participating atoms should satisfy

$$m_F(a) + m_F(c) = m_F(b) + m_F(d) \tag{36}$$

(see Fig. 8) and thus, the only m_F conserving processes (collisions) are (see Fig. 9)

(i) $a,c \to b,d$, and vice versa. This yields terms such as $c_n^\dagger a_n^\dagger b_n d_{n+1} + d_{n+1}^\dagger b_{n+1}^\dagger a_{n+1} c_{n+2}$.

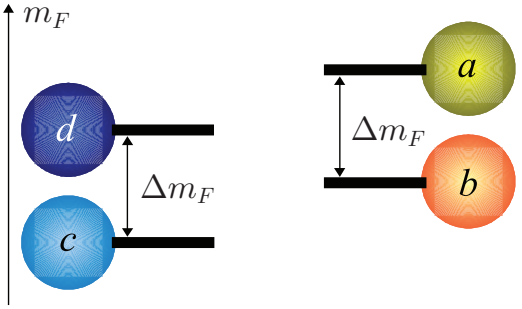

FIG. 8. (Color online) A schematic plot of the required choice of m_F values. As in Eq. (36), the equal spacing between Δm_F the m_F of bosons (a,b on the right) and fermions (c,d on the left) is required to allow only gauge-invariant collisions.

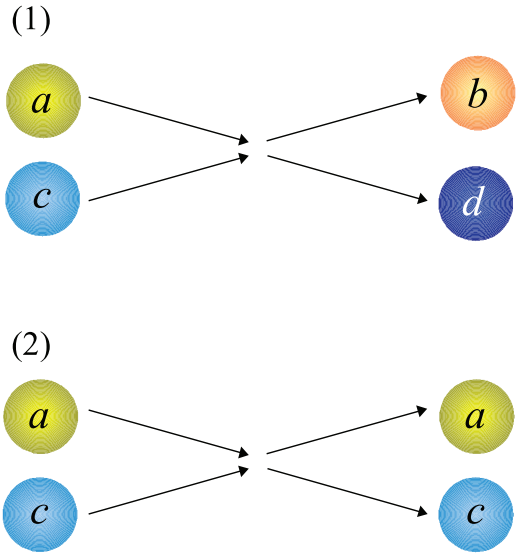

FIG. 9. (Color online) Schematic examples of the two types of possible Boson-Fermion scattering processes (collisions) along a link: (i) species-changing and (ii) non-species-changing. Both of them conserve total m_F and thus are gauge invariant.

(ii) $a,c \to a,c$, and the same with b,d. This results in terms such as $c_n^\dagger c_n (a_k^\dagger a_k + b_k^\dagger b_k)$ where the link k starts or ends in the vertex n. As all this terms $a_k^\dagger a_k + b_k^\dagger b_k = N_0$, one eventually gets a contribution, which is proportional to the constant number of fermions, an ignorable constant in the energy.

The first term is the desired gauge-invariant interaction. To see that, just perform the canonical transformation

$$\begin{pmatrix} a_n \\ b_n \end{pmatrix} \to \sigma_x^n \begin{pmatrix} a_n \\ b_n \end{pmatrix} \tag{37}$$

and redefine the scattering coefficients in H_{sc}, to obtain[5]

$$H_{int} = \frac{\epsilon}{\sqrt{\ell(\ell+1)}} \sum_n (\psi_n^\dagger L_{+,n} \psi_{n+1} + \text{H.c.}) \tag{38}$$

This Hamiltonian is especially interesting (although not realizable) in the limit $N_0 \to \infty$. In that case, $\ell \to \infty$, and thus always $m \ll \ell$. Thus $L_\pm$, in this limit, are unitary operators

$$\frac{L_\pm}{\sqrt{\ell(\ell+1)}}|\ell m\rangle = \sqrt{1 - \frac{m(m\pm 1)}{\ell(\ell+1)}}|\ell, m\pm 1\rangle \underset{\ell\to\infty}{\longrightarrow} |\ell, m\pm 1\rangle \tag{39}$$

and thus we get that $\frac{L_\pm}{\sqrt{\ell(\ell+1)}}$ approaches in this limit a unitary operator (pure phase), as in the Kogut-Susskind model. Another way to see it is to consider that in this case the bosons form BECs. For $N_0 \gg 1$, one can approximate $a_n \approx \sqrt{\frac{N_0}{2}} e^{-i\theta_n^a} = \sqrt{\ell} e^{-i\theta_n^a}$, etc. ($m \ll \ell$ and thus $N_a - N_b \ll N_0$)

[5]One can also introduce different phases to H_{int}, as is sometimes done, by using another canonical transformation, of the form $\psi_n \to (-i)^n \psi_n$.

and it is reasonable to approximate $N_a \approx \frac{N_0}{2}, N_b \approx \frac{N_0}{2}$. Then,

$$\frac{1}{\sqrt{\ell(\ell+1)}}\psi_n^\dagger a_n^\dagger b_n \psi_{n+1} \approx \psi_n^\dagger e^{i\phi_n}\psi_{n+1}, \tag{40}$$

where $\phi_n = \theta_n^a - \theta_n^b$. This is similar to the mapping of [10].

B. $\mathbb{Z}_N$ elementary interactions

Now we turn to the construction of the elementary interactions of another Abelian LGT theory, but this time with a *discrete* gauge group, $\mathbb{Z}_N$. Besides being an interesting gauge theory on its own, we consider its quantum simulation due to the fact that here, in order to simulate the exact theory, with exactly unitary gauge operators in the elementary interactions, we need a finite number of degrees of freedom, which makes this theory more tempting to realize, unlike the cQED case, in which we only approximated the unitary interactions by angular momentum ladder operators.

Although we use the same general techniques of angular momentum conservation, one must note that in this case it is not enough. This is due to the fact that the $\mathbb{Z}_N$ Q operators are cyclic (see Sec. II B2 details), forming an Escher's staircase [64], and thus regular angular momentum conservation is not sufficient. Therefore we use on top of the angular momentum conservation hybridization of states, and make use of auxiliary bosonic levels.

For simplicity, we describe here the construction of elementary interactions of the $\mathbb{Z}_3$ case in $2+1$ dimensions, but it can be easily generalized for larger N and higher dimensions. We do not consider the $1+1$ dimensional theory as our fermions are not $\mathbb{Z}_3$ charges, but rather auxiliary particles, which shall be traced out in the derivation of plaquette interactions (see Sec. VI B): this point will become clear in the following derivation of the elementary interactions.

For obtaining the elementary interactions of $\mathbb{Z}_3$, we need, on each link, six fermionic species: four regular hyperfine levels, which we label $\{a_i\}_{i=1}^4$, and two auxiliary levels $\{c_i\}_{i=2}^3$ (see Fig. 10). The vertices, unlike before, are occupied by bosons, whose annihilation operators are $\psi_{\mathbf{n}}, \chi_{\mathbf{n}}$ which, due to energy shifts, can occupy alternating vertices (like the fermions in the Schwinger model simulation, and thus the use of fermionic letters). The vertex bosons are subject to a hardcore constraint,

$$H_c = \lambda \sum_v N_v (N_v - 1), \tag{41}$$

where N_v is the total number of bosons on the vertex v. Initially all the vertices are filled by only one boson, even vertices with ψ and odd with χ.

The hyperfine levels of the atoms should satisfy the relation

$$m_f(\psi) + m_f(a_i) = m_f(\chi) + m_f(a_{i+1}) \tag{42}$$

for $i \in \{1,2,3\}$ (see Fig. 10). The c levels should be picked far enough energetically, such that they will not be involved in any link-species-changing process. Thus, the boson-fermion scattering terms will be of the two following forms:

(i) Collisions with no change of species.

$$H_\alpha = \alpha \sum_{\langle l,v\rangle} N_v N_l, \tag{43}$$

where $\langle l,v\rangle$ are neighboring links and vertices, N_v is the total number of fermions on the vertex v and N_l—the total number of bosons on the link l. We prepare the system initially with $N_l = 1$. This is not changed by any interaction, and thus this term turns out to be proportional to the total number of fermions in the system, an ignorable constant.

(ii) Collisions with a change of species. For even vertices (emanating from an even $\mathbf{n}$), we have

$$2\epsilon \sum_k \left(\psi_{\mathbf{n}}^\dagger \sum_{i=1}^3 a_{i,\mathbf{n},k}^\dagger a_{i,\mathbf{n},k} \chi_{\mathbf{n}+\hat{\mathbf{k}}} + \text{H.c.} \right) \tag{44}$$

For odd links, one has to replace $\psi \leftrightarrow \chi$ in the equation above. However, we can perform a canonical transformation, inverting the names of hyperfine levels on odd links, and then have them described by the same sort of interaction [compare to the canonical transformation of (37)]. After doing that we call, formally, all the vertex bosons ψ and obtain

$$H_{\text{int}} = 2\epsilon \sum_{\mathbf{n},k} \left(\psi_{\mathbf{n}}^\dagger \sum_{i=1}^3 a_{i,\mathbf{n},k}^\dagger a_{i,\mathbf{n},k} \psi_{\mathbf{n}+\hat{\mathbf{k}}} + \text{H.c.} \right) \tag{45}$$

Since there is only one boson on each link, other boson-boson scattering processes are irrelevant.

We also introduce, using Raman lasers (see Fig. 10), for each link, the following bosonic tunneling Hamiltonian, within each link:

$$\begin{aligned} H_R = {} & (\Delta_1+\delta_1)(a_1^\dagger a_1 + a_4^\dagger a_4) + (\Omega_1+\omega_1)(a_1^\dagger a_4 + a_4^\dagger a_1) \\ & + (\Delta_2+\delta_2)(a_2^\dagger a_2 + c_2^\dagger c_2) + (\Omega_2+\omega_2)(a_2^\dagger c_2 + c_2^\dagger a_2) \\ & + (\Delta_3+\delta_3)(a_3^\dagger a_3 + c_3^\dagger c_3) + (\Omega_3+\omega_3)(a_3^\dagger c_3 + c_3^\dagger a_3). \end{aligned} \tag{46}$$

Note that the $a_1 \leftrightarrow a_4$ process involves a three-unit angular momentum change, and thus it should be mediated by three photons.

We make Δ_i, Ω_i the largest energy scales in the total Hamiltonian, and thus it will be reasonable to diagonalize H_R first, and obtain a hybridization of the couples of states coupled

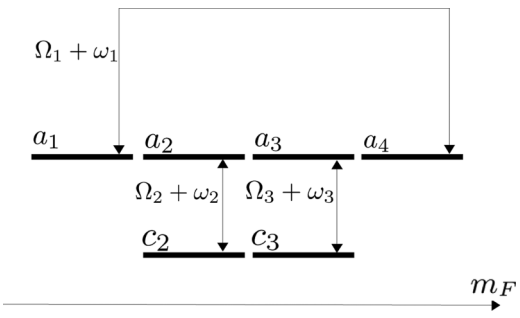

FIG. 10. A schematic plot of the required choice of m_F values, for the four regular levels $\{a_i\}_{i=1}^4$, and the two auxiliary levels $\{c_i\}_{i=2}^3$ as in Eq. (42). Note that this plot shows m_F only; not all the processes are available, only the gauge-invariant ones, as in (45). Some processes are eliminated due to energy shifts, which are not drawn in this figure. Also schematically shown (by arrows) are the lasers connecting coupled of levels in H_R (46).

with lasers, in the form of a Bogolyubov transformation

$$b_1^\dagger = \frac{1}{\sqrt{2}}(a_1^\dagger + a_4^\dagger); \quad d_1^\dagger = \frac{1}{\sqrt{2}}(a_1^\dagger - a_4^\dagger)$$
$$b_2^\dagger = \frac{1}{\sqrt{2}}(a_2^\dagger + c_2^\dagger); \quad d_2^\dagger = \frac{1}{\sqrt{2}}(a_2^\dagger - c_2^\dagger) \tag{47}$$
$$b_3^\dagger = \frac{1}{\sqrt{2}}(a_3^\dagger + c_3^\dagger); \quad d_3^\dagger = \frac{1}{\sqrt{2}}(a_3^\dagger - c_3^\dagger).$$

By setting $\Omega_i = -\Delta_i$, we obtain the diagonalized form

$$H_R = 2\sum_{i,\mathbf{n},k} \Delta_i d_{i,\mathbf{n},k}^\dagger d_{i,\mathbf{n},k} + (\delta,\omega \text{ terms}) \tag{48}$$

and since we choose Δ to be very large, we can disregard, effectively, the d_i modes. Plugging the Bogolyubov transformation (47) into H_{int}, disregarding the d modes, we get

$$H_{\text{int}} = \epsilon \sum_{\mathbf{n},k} (\psi_{\mathbf{n}}^\dagger Q_{\mathbf{n},k} \psi_{\mathbf{n}+\hat{\mathbf{k}}} + \text{H.c.}), \tag{49}$$

where

$$Q = b_1^\dagger b_2 + b_2^\dagger b_3 + b_3^\dagger b_1 \tag{50}$$

is the unitary Q of $\mathbb{Z}_3$ (see Sec. II B2 for details). Thus H_{int} is the desired $\mathbb{Z}_3$ elementary interaction. Note, however, that the vertex bosons do not represent $\mathbb{Z}_3$ charges, and thus this method can only be used to generate auxiliary particles, and not dynamic charges.

Finally, we have to represent the electric part, H_E. Plugging the new modes into H_R, we get

$$H_R = \sum_{i,\mathbf{n},k} ((\delta_i + \omega_i) b_{i,\mathbf{n},k}^\dagger b_{i,\mathbf{n},k} + (\delta_i - \omega_i) d_{i,\mathbf{n},k}^\dagger d_{i,\mathbf{n},k}). \tag{51}$$

Then, setting $\delta_i = \omega_i$, one gets

$$H_R = 2\sum_{i,\mathbf{n},k} \delta_i b_{i,\mathbf{n},k}^\dagger b_{i,\mathbf{n},k}. \tag{52}$$

We identify

$$P + P^\dagger = 2\sum_m \cos(m\delta)\, b_m^\dagger b_m \tag{53}$$

(where $\delta = 2\pi/N$), and thus, for $\mathbb{Z}_3$,

$$H_E = \frac{\mu}{2} \sum_{\mathbf{n},k} (b_{1,\mathbf{n},k}^\dagger b_{1,\mathbf{n},k} - 2 b_{2,\mathbf{n},k}^\dagger b_{2,\mathbf{n},k} + b_{3,\mathbf{n},k}^\dagger b_{3,\mathbf{n},k}). \tag{54}$$

Set $\delta_1 = \delta_3 = \frac{\mu}{2}$ and $\delta_2 = -\mu$ and obtain, neglecting constants,

$$H = H_C + H_R + H_{\text{int}} = H_C + H_E + H_{\text{int}}. \tag{55}$$

This is the fundamental Hamiltonian, with *unitary* elementary interactions, from which we can now construct effectively the $\mathbb{Z}_3$ Hamiltonian with plaquette terms.

Note that in order to obtain the correct interactions, one must use several Feshbach resonances. Their number can be reduced, if one generalizes the Hamiltonian to include some energy difference between $a_1^\dagger a_1$ and $a_4^\dagger a_4$, and also for the other two couples of hybridized states. Then one can introduce a few more parameters to play with, and reduce the number of required Feshbach resonances.

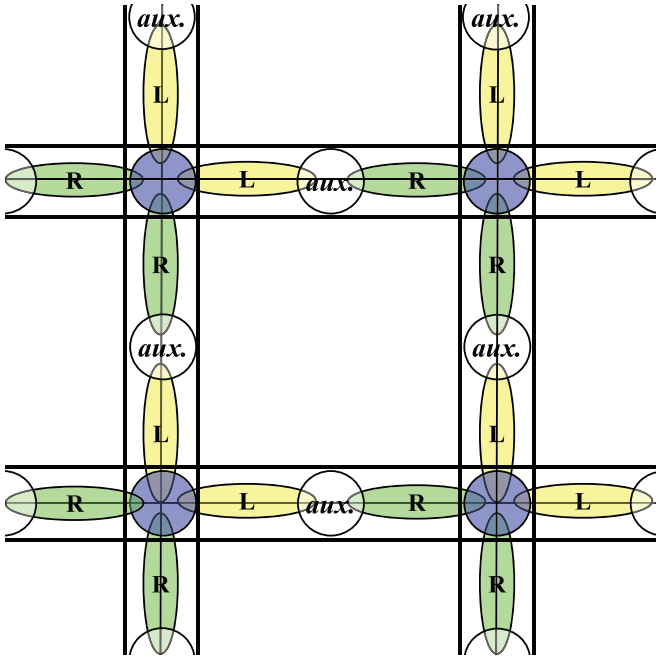

FIG. 11. (Color online) The lattice structure required for elementary SU(N) interactions. Each link is decomposed to left (L) and right (R) parts. It is constructed from two links of the optical lattice, tailored together by a constrained satisfied by auxiliary (aux) fermions in the middle.

Also, note that in order to generalize to $\mathbb{Z}_N$ for $N > 3$, one must have $2N$ bosonic species on each link, $\{a_i\}_{i=1}^{N+1}$ and $\{c_i\}_{i=2}^{N}$. The hybridization method is the same, with coupling between a_1 and a_N, and a_i and c_i for $i \in \{2,\ldots,N\}$.

C. SU(N) Yang-Mills elementary interactions

We shall also refer to the fundamental Hamiltonian for SU(N) elementary interactions. There, the system is more complicated, and many atomic species are required. Due to the decomposition of a single link to two parts (left and right, see Sec. II B3), this richer Hilbert space requires the construction of a single link of what was two separate links for the Abelian theories, i.e., a simulating link is effective, and it is constructed from two atomic links, tailored by some constrained auxiliary fermions between them (see Fig. 11).

We shall briefly review the ideas of Ref. [17], in which a non-Abelian quantum simulator for a $1+1$ dimensional SU(2) lattice gauge theory was suggested. This simulation method utilizes prepotentials [56], in which the group degrees of freedom are constructed out of prepotentials: harmonic oscillators, or, in our case, bosonic species. This enables a bosonic representation of the full Kogut-Susskind model. Fermionic representations are available too, using the link model [52,53], however, they correspond to truncated gauge theories, with finite local Hilbert spaces, from which one obtains the full theories only in the continuum limit.

As explained in Sec. II B3, and in Fig. 11, each link is decomposed into two parts, the left and the right, and hence simulated by two links of the optical lattice. In each of the link's parts, four bosonic species reside: a_1,a_2,c_1,c_2 on the left, and b_1,b_2,d_1,d_2 on the right. The a,b species

are the gauge field degrees of freedom, forming, using a Schwinger representation, the left and right generators of the group, respectively,

$$L_a = \frac{1}{2}\sum_{k,l} a_k^\dagger (\sigma_a)_{lk} a_l; \quad R_a = \frac{1}{2}\sum_{k,l} b_k^\dagger (\sigma_a)_{kl} b_l \tag{56}$$

satisfying the required algebra of the group [Eq. (26)], with $j = \frac{N_L}{2} = \frac{N_R}{2}$ and the Casimir operators $\mathbf{L}^2 = \frac{N_L}{2}(\frac{N_L}{2}+1)$, $\mathbf{R}^2 = \frac{N_R}{2}(\frac{N_R}{2}+1)$ (where $N_L \equiv a_1^\dagger a_1 + a_2^\dagger a_2$ and $N_R \equiv b_1^\dagger b_1 + b_2^\dagger b_2$, satisfying the constraint $N_L = N_R$).

From these, in the prepotential method, one may construct the left and right matrices (of operators), in the fundamental representation,

$$\begin{aligned} U_L &= \frac{1}{\sqrt{N_L+1}}\begin{pmatrix} a_1^\dagger & -a_2 \\ a_2^\dagger & a_1 \end{pmatrix}; \\ U_R &= \begin{pmatrix} b_1^\dagger & b_2^\dagger \\ -b_2 & b_1 \end{pmatrix}\frac{1}{\sqrt{N_R+1}}; \end{aligned} \tag{57}$$

and obtain the group element on the link, in the fundamental representation,

$$U = U_L U_R \tag{58}$$

satisfying the required commutation relations (25). The c,d species are prepared in coherent states (Bose-Einstein condensate) $|\alpha\rangle$, where $\alpha \in \mathbb{R}, \alpha \gg 1$.

Let us denote the real spinors by ψ and the auxiliary ones, connecting between two links, which will form one link in the simulated theory, χ. Then, by properly choosing the hyperfine levels of all the atoms (see the supplemental material of Ref. [17] for an explicit example), and tuning the scattering coefficients, we get the angular-momentum-conserving interaction Hamiltonian for elementary interactions,

$$\begin{aligned} H_{\rm int} = \frac{\epsilon}{2^{1/4}\alpha}\sum_{n,i,j} &((\psi_n^\dagger)_i (\tilde{W}_{L,n})_{ij} (\chi_n)_j \\ &+ (\chi_n^\dagger)_i (\tilde{W}_{R,n})_{ij} (\psi_{n+1})_j + \text{H.c.}), \end{aligned} \tag{59}$$

where

$$\tilde{W}_L = \begin{pmatrix} a_1^\dagger c_1 & -a_2 c_2^\dagger \\ a_2^\dagger c_2 & a_1 c_1^\dagger \end{pmatrix}; \quad \tilde{W}_R = \begin{pmatrix} b_1^\dagger d_1 & b_2^\dagger d_2 \\ -b_2 d_2^\dagger & b_1 d_1^\dagger \end{pmatrix} \tag{60}$$

and we label the two links from which the effective link n (emanating from the real vertex n) will be generated by n,L and n,R.

The use of condensates for the auxiliary bosonic species allow us to replace c_i, d_i by α, and since $\alpha \gg 1$ we can approximately do the same for $c_i^\dagger, d_i^\dagger$, and one effectively obtains the Hamiltonian

$$\begin{aligned} H_f = \frac{\epsilon}{2^{1/4}}\sum_{n,i,j} &(\sqrt{N_{L,n}+1}(\psi_n^\dagger)_i (U_{L,n})_{ij} (\chi_n)_j \\ &+ (\chi_n^\dagger)_i (U_{R,n})_{ij} (\psi_{n+1})_j \sqrt{N_{R,n}+1} + \text{H.c.}). \end{aligned} \tag{61}$$

The auxiliary fermions are constrained by the large-scale energy constraint

$$H_\chi = \lambda \sum_n \chi_n^\dagger \chi_n. \tag{62}$$

If initially the system does not contain any χ fermions, and λ is the largest energy scale, we can obtain, using second-order perturbation theory, an effective Hamiltonian, tailoring the two sides of each link, of the form

$$H_{\rm int}^{\rm eff} = \frac{\epsilon_{\rm eff}}{\sqrt{2}}\sum_n (\psi_n^\dagger \sqrt{N_{L,n}+1} U_n \sqrt{N_{R,n}+1}\psi_{n+1} + \text{H.c.}) \tag{63}$$

These are the elementary interactions of SU(2). However, note that the bosonic link operators are not unitary, i.e., we have $\sqrt{N_{L,n}+1}U_n\sqrt{N_{R,n}+1}$ rather than U_n. In spite of that, as will be explained in the next section, one can still get qualitatively the same physics, in the appropriate parameter regime.

Also note that although the full link is obtained effectively, the gauge invariance is still fundamental and it is constructed out of two already gauge-invariant building blocks: the left and right parts. The prepotentials method can of course be generalized to SU(N) gauge theories with $N > 2$ [65–67], and serve as a base for obtaining the elementary interactions in a similar manner.

V. 1 + 1 DIMENSIONAL MODELS

Having the elementary interactions in hand, we can now construct complete quantum simulations of $1+1$ dimensional gauge theories with dynamic fermions. This can be done for cQED, but not for $\mathbb{Z}_N$, as we do not discuss discrete charges in this paper. A proposal based on our method for the simulation of $1+1$ dimensional SU(2) theory has already been suggested in Ref. [17], and we shall review it here as well.

A. Quantum simulation of the Schwinger model

Let us start with the a quantum simulation of the Schwinger model: a $1+1$ dimensional Abelian gauge theory (QED) coupled to dynamical fermions (see Appendix A2). The solvable Schwinger model involves massless fermions. We discuss also the more general massive case. Being $1+1$ dimensional, this system does not involve any plaquette interactions, and thus we already have all the interactions we need.

Besides $H_{\rm int} + H_M$ [Eqs. (35) and (38)], we also need the electric Hamiltonian. $H_E = \frac{g^2}{2}\sum_{n,k} E_n^2 = \frac{g^2}{2}\sum_n L_{z,n}^2$, or, in the atomic terms,

$$H_E = \frac{g^2}{8}\sum_n \left(N_{a,n}^2 + N_{b,n}^2 - 2N_{a,n}N_{b,n}\right). \tag{64}$$

This is exactly obtained from the boson-boson scattering terms of (31). These processes, of course, conserve the total m_F in collisions. The minus sign in the interaction may be avoided as well, thanks to the constant N_0: one could, instead, use the Hamiltonian

$$\begin{aligned} H_E' = &\left(\alpha + \frac{g^2}{8}\right)\sum_n \left(N_{a,n}^2 + N_{b,n}^2\right) \\ &+ \left(2\alpha - \frac{g^2}{4}\right)\sum_n N_{a,n}N_{b,n}, \end{aligned} \tag{65}$$

which is just H_E, plus a constant in the energy, $\alpha\sum_n(N_{a,n} + N_{b,n}) = \alpha\sum_n N_0^2$, which is, of course, ignorable. Linear terms

in the total number of bosons on a link (from H_{sc} and H_0) yield ignorable constants as well.

Thus we get the Hamiltonian

$$H = H_E + H_M + H_{\text{int}} \tag{66}$$

describing the dynamics of a U(1) spin-gauge theory with dynamic fermions [13,15] in $1+1$ dimensions.

For a finite N_0, one gets qualitatively the features of the model. As N_0 (or ℓ) increases, the model becomes more accurate. The phase approximation can be made for condensates, in which one must make sure that three-body interactions are negligible. This can be assumed if the condensate is made in the shape of a tube, whose axis is perpendicular to the link, increasing the number of particles but reducing their density.

Thus we have shown how to simulate a $1+1$-d cQED with dynamic staggered fermions (lattice Schwinger model) using ultracold atoms, with an exact gauge symmetry and no use of perturbation theory and effective low-energy considerations unlike in previous suggestions.

B. Quantum simulation of 1 + 1 dimensional SU(2) gauge theory

Having also the SU(2) elementary interactions in hand, one can obtain a $1+1$ dimensional simulation of an SU(2) gauge theory.

On top of the elementary interactions (63), one shall include as well the electric and matter Hamiltonians,

$$H_E = \frac{1}{2}\sum_n \left[g_L \frac{N_{L,n}}{2}\left(\frac{N_{L,n}}{2}+1\right) + g_R \frac{N_{R,n}}{2}\left(\frac{N_{R,n}}{2}+1\right)\right] \tag{67}$$

with $g_R + g_L = g^2$, and

$$H_M = M\sum_n (-1)^n \psi_n^\dagger \psi_n. \tag{68}$$

This enables a simulation of the dynamics of the vacuum of the theory, up to fifth-order perturbation theory in $H_{\text{int}}^{\text{eff}}$ (63). See Ref. [17] and its supplemental material for further details.

VI. INTERACTIONS ON PLAQUETTES: THE LOOP METHOD

In the next step, we would like to generalize our discussion to further dimensions. However, the $1+1-d \to 2+1-d$ transition is nontrivial, since the plaquette terms must be introduced, and, as explained, they are not a fundamental part of the atomic Hamiltonian. In previous proposals, the plaquette terms have been obtained effectively, by constraining the Gauss's law, and introducing gauge invariance effectively, as a symmetry of the low-energy sector. In this section, we show yet another way to get the plaquette terms. Although in what we shall describe the plaquettes will be obtained effectively as well, it is believed to be much more robust than the previous methods, since although we get the plaquette terms effectively, gauge invariance is fundamental as described in the previous sections: the building blocks, which are elementary interactions, are already gauge invariant. This is called the loop method.

The idea is as follows. First, extend the scheme for $1+1$ simulations to more dimensions (which already serves as a simulation for the extreme strong limit). Then, treat the fermions as auxiliary particles, by adding a constraint, which forces them to occupy only certain vertices (exactly one vertex belonging to each plaquette of the lattice), H_C instead of H_M (the auxiliary particles do not have to be massive). H_{int}, operating on states satisfying this constraint, will take us out of the right sector. Thus it would be reasonable to construct an effective theory in the ground sector of this constrained Hamiltonian, and then, in fourth order (operating with elements of H_{int} around each plaquette) one obtains the required interaction. Remarkably, these fourth-order terms are unnecessarily weak: as it turns out—and will be clarified throughout the following derivations—the relevant leading order is either the second order (for Abelian theories, with no third order) or the fourth one (for non-Abelian theories), and thus the perturbative parameter should be small only to order 2 or 4.

The nature of auxiliary particles varies from one gauge theory to another, and depends on the gauge group. We shall describe, separately, the methods of constructing such simulations for three different gauge theories: U(1), $\mathbb{Z}_N$, and SU(N). For the sake of simplicity, we consider the $2+1$-d case. However, at least by geometric means, the constructions for higher dimensions are similar.

As a final general remark, before getting into specific theories, one should note that in this method the fermions are traced out and eventually a pure-gauge theory is obtained. Such theories, in dimensions higher than $1+1$, are interesting on their own, without including dynamic fermions; However, one could also include more fermionic species, not subjected to the plaquette constraint described above, which will serve as dynamical matter. This is discussed in Sec. VIII.

A. cQED plaquettes

Our first example of effective derivation of plaquettes in the loop method will be for the case of cQED, a generalization of the Schwinger model simulation described in the previous section. For that, we start with a similar system to the one described for $1+1$-d, but with two spatial dimensions instead of one. Thus, the system is described by the Hamiltonian (66), generalized to two dimensions, i.e., all the vertex indices become vectors $n \to \mathbf{n} \in \mathbb{Z}^2$ and the links are now identified by two indices: $\mathbf{n}$ and the direction $k \in \{1,2\}$. The electric part of the Hamiltonian is

$$H_E = \frac{g^2}{2}\sum_{\mathbf{n},k} (E_{\mathbf{n},k})^2. \tag{69}$$

We introduce another set of fermions, $\chi_{\mathbf{n}}$, which behave like the $\psi_{\mathbf{n}}$s (including the same interactions with the bosons). At this stage, for the sake of illustration of the method for obtaining plaquettes, we assume that the bosonic link operators are really unitary ($N_0 \to \infty$), i.e., we work with the elementary interactions

$$\begin{aligned} H_{\text{int}} &= \epsilon \sum_{\mathbf{n},k} (\psi_{\mathbf{n}}^\dagger U_{\mathbf{n},k} \psi_{\mathbf{n}+\hat{\mathbf{k}}} + \chi_{\mathbf{n}}^\dagger U_{\mathbf{n},k} \chi_{\mathbf{n}+\hat{\mathbf{k}}} + \text{H.c.}) \\ &= \epsilon \sum_{\mathbf{n},k} (\psi_{\mathbf{n}}^\dagger e^{i\phi_{\mathbf{n},k}} \psi_{\mathbf{n}+\hat{\mathbf{k}}} + \chi_{\mathbf{n}}^\dagger e^{i\phi_{\mathbf{n},k}} \chi_{\mathbf{n}+\hat{\mathbf{k}}} + \text{H.c.}). \end{aligned} \tag{70}$$

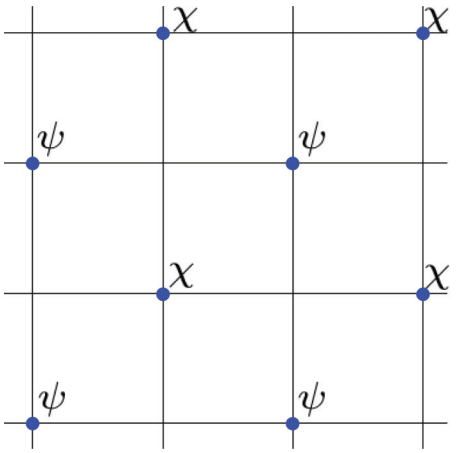

FIG. 12. (Color online) The preferred vertices of the ψ,χ fermions, in the even vertices, according to the constraint set by H_C [Eq. (71)]. Each plaquette contains exactly such two vertices, one of ψ and one of χ.

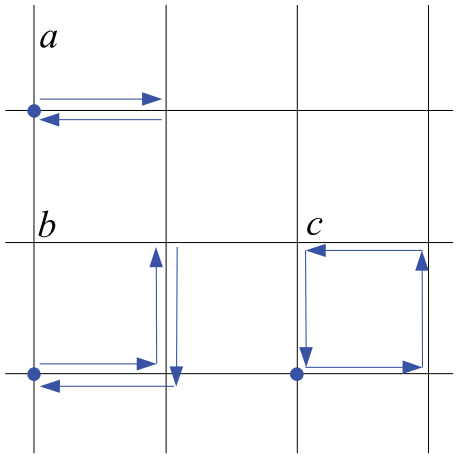

FIG. 13. (Color online) Examples for jumping of auxiliary fermions from their preferred vertices and back, (a) in the second order of $H_{\rm int}$, (b), (c) in the fourth order of $H_{\rm int}$, where (c) forms the plaquette interactions.

Note that the hyperfine levels of the two χ species must be chosen carefully, such that $\chi-\psi$ remain separate in $H_{\rm int}$ and no mixing interactions can occur. The difference between the types of fermions is found in a constraint we add on the fermions,

$$H_C=-\lambda\sum_{\mathbf{n}}(F_\psi(\mathbf{n})\psi^\dagger_{\mathbf{n}}\psi_{\mathbf{n}}+F_\chi(\mathbf{n})\chi^\dagger_{\mathbf{n}}\chi_{\mathbf{n}}),\qquad(71)$$

where F_ψ is zero everywhere, unless where both the indices n_1,n_2 are even, where it takes the value of 1, and F_χ is zero everywhere, unless where both the indices n_1,n_2 are odd, where it is 1. If we define both these types of vertices as even ones, we see that H_C puts an energy penalty for each species not being in its specific preferred type of an even vertex (see Fig. 12). H_M is of course unnecessary here, as explained in the introduction of this section.

We denote the ground sector of H_C as $\mathcal{M}_0$, and wish to work in this subspace. Thus, the system has to be initially prepared in a state where all the fermions occupy only even vertices (the opposite to the Dirac sea case for dynamic fermions). Note that since H is gauge invariant, and we initially prepare the system in a gauge-invariant state, the dynamics will leave the state gauge invariant and thus we choose to specifically work in $\mathcal{M}\subset\mathcal{M}_0$, which is the set of gauge-invariant states inside $\mathcal{M}_I$. As λ is the largest energy scale, we derive an effective Hamiltonian within $\mathcal{M}_0$; we shall construct a low-energy effective theory, which includes the plaquette interactions. In order to do that we use time-independent perturbation theory, following the notations of Ref. [36].

1. First- and second-order contributions

Denote $\mathcal{P}_0$ as the projection operator to $\mathcal{M}_0$, and define $H_1=H_E+H_{\rm int}$ and

$$\mathcal{K}=\sum_{|\alpha\rangle\notin\mathcal{M}_0}\frac{|\alpha\rangle\langle\alpha|}{E_C(\alpha)-E_C(0)},\qquad(72)$$

where E_C is the eigenvalue of H_C, and thus $E_C(0)=0$. Also, for the convenience of series expansions, denote $\mu\equiv\frac{g^2}{2}$.

The first-order term in the effective expansion is $H^{(1)}_{\rm eff}=\mathcal{P}_0H_1\mathcal{P}_0=H_E$. In second order, we have $H^{(2)}_{\rm eff}=-\mathcal{P}_0H_1\mathcal{K}H_1\mathcal{P}_0$. Here, in $\mathcal{K}$, only H_1 will contribute, taking to (and from) intermediate states $|\alpha\rangle$ with $E_C(\alpha)=\lambda$ (the constraint is violated only for one fermion). The contributions will be only of double operations of H_1 on the same link [see Fig. 13(a)], and due to the unitarity of the interactions will lead (within $\mathcal{M}_0$) to a constant in the energy, which is ignorable.

2. Third-order contributions

The third-order contribution takes the form $H^{(3)}_{\rm eff}=\mathcal{P}_0H_1\mathcal{K}H_1\mathcal{K}H_1\mathcal{P}_0-\frac{1}{2}\{\mathcal{P}_0H_1\mathcal{K}^2H_1\mathcal{P}_0,\mathcal{P}_0H_1\mathcal{P}_0\}$. The second (anticommutator) term is just a combination of the first- and second-order terms, which will result in $-\mathcal{N}\frac{\epsilon^2}{\lambda^2}H_E$, where $\mathcal{N}$ is the number of links.

The first term is nonzero only for the combination $\mathcal{P}_0H_{\rm int}\mathcal{K}H_E\mathcal{P}_0\mathcal{K}H_{\rm int}\mathcal{P}_0$. Here, as in the second order, $E_C(\alpha)=\lambda$. These terms will vanish, unless we consider, as in the second order, double operation of $H_{\rm int}$ on the same link. Define a positive link if it starts on an even vertex, and a negative link if it ends there. Since only states where even vertices are occupied belong to $\mathcal{M}_0$, only the part $\psi^\dagger_{\mathbf{n}+\hat{\mathbf{k}}}U^\dagger_{\mathbf{n},k}\psi_{\mathbf{n}}$ of $H_{\rm int}$ acting on $\mathcal{M}_0$ will give rise to a nonzero contribution, and thus in the final operation, the contribution will come from $\psi^\dagger_{\mathbf{n}}U_{\mathbf{n},k}\psi_{\mathbf{n}+\hat{\mathbf{k}}}$ (and similarly for χ). For negative links, only the opposite processes contribute. Thus, for each positive link $\mathbf{n},k$ we get the contribution

$$\frac{\epsilon^2}{\lambda^2}UH_EU^\dagger=\frac{\epsilon^2}{\lambda^2}H_E-\frac{2\mu\epsilon^2}{\lambda^2}E_{\mathbf{n},k}+\mathcal{D},\qquad(73)$$

where $\mathcal{C}$ is the same constant as in the other third-order contribution, and $\mathcal{D}$ is another constant. Similarly, for negative links we get

$$\frac{\epsilon^2}{\lambda^2}U^\dagger H_EU=\frac{\epsilon^2}{\lambda^2}H_E+\frac{2\mu\epsilon^2}{\lambda^2}E_{\mathbf{n},k}+\mathcal{D}.\qquad(74)$$

The $\mathcal{D}$ parts can be ignored, as constants, and after summing on all the links (remember that each link is a neighbor of exactly

one even vertex, and thus it is either positive or negative) we get a cancellation of the $\frac{\epsilon^2}{\lambda^2}H_E$ parts, and eventually we are left, for every even $\mathbf{n}$, with $-\frac{2\mu\epsilon^2}{\lambda^2}\mathrm{div}_{\mathbf{n}}E$, where the discrete divergence is $\mathrm{div}_{\mathbf{n}}E = (E_{\mathbf{n},1} + E_{\mathbf{n},2} - E_{\mathbf{n}-\hat{\mathbf{1}},1} - E_{\mathbf{n}-\hat{\mathbf{2}},2}) = \text{const.}$ within $\mathcal{M}_0$ by Gauss's law (in case of no dynamic charges). Thus all the third-order contributions are constants and we disregard them.

3. *Fourth-order contributions*

In fourth order, there are much more contributions. The ones involving H_E yield mostly ignorable constants based on Gauss's law, as in the third order. There are some possible fourth-order processes involving only H_{int} on two links, corresponding to back-and-forth hopping of fermions [see Fig. 13(b)], which result in constants due to the unitarity of interactions, as in the second order.

The nonconstant contributions are of two types. The terms involving H_E yield a renormalization to the electric Hamiltonian, of the form

$$\delta H_E = \frac{\mu^2\epsilon^2}{\lambda^3}\sum_{\mathbf{n},k}(E_{\mathbf{n},k})^2. \tag{75}$$

This is the reason for the inclusion of χ fermions. Otherwise, we would have got such renormalizations only for links which are neighbors of the preferred vertices of ψ.

The other type contributions are the anticipated plaquette interactions. These arise from the contribution $-\mathcal{P}_0 H_{\mathrm{int}}\mathcal{K}H_{\mathrm{int}}\mathcal{K}H_{\mathrm{int}}\mathcal{K}H_{\mathrm{int}}\mathcal{P}_0$, where the four operations of H_{int} cause a fermion to hop from its rest vertex, around a plaquette, and back to the original place, and thus forming the desired Hamiltonian terms [see Fig. 13(c)]. Each plaquette operator is divided into two different orientations (clockwise and counterclockwise). Each orientation is obtained twice, because it has to start (and finish) in an even vertex, and each plaquette contains two such vertices, i.e., each plaquette interaction is obtained once using ψ and once using χ. Altogether we get the required

$$\begin{aligned} H_B &= -\frac{2\epsilon^4}{\lambda^3}\sum_{\mathbf{n}}(U_{\mathbf{n},1}U_{\mathbf{n}+\hat{\mathbf{1}},2}U^{\dagger}_{\mathbf{n}+\hat{\mathbf{2}},1}U^{\dagger}_{\mathbf{n},2} + \mathrm{H.c.}) \\ &= -\frac{4\epsilon^4}{\lambda^3}\sum_{\mathbf{n}}\cos(\phi_{\mathbf{n},1} + \phi_{\mathbf{n}+\hat{\mathbf{1}},2} - \phi_{\mathbf{n}+\hat{\mathbf{2}},1} - \phi_{\mathbf{n},2}) \end{aligned} \tag{76}$$

and eventually the Abelian Kogut-Susskind Hamiltonian is obtained

$$H_{\mathrm{eff}} = H_E + \delta H_E + H_B. \tag{77}$$

One may claim that the plaquette interactions are negligible here, since they are obtained in fourth-order perturbation theory. However, note that all the terms in the effective Hamiltonian involving ϵ actually involve ϵ^2; only even orders contribute (since one can return to $\mathcal{M}_0$ only with an even number of H_{int} operations). Thus, it is sufficient to demand $\epsilon^2 \ll \lambda^2$, rather than $\epsilon \ll \lambda$.

Dynamical fermions may be introduced through the inclusion of another set of fermions, with its own H_{int} and H_M, and without any constraint (see Sec. VIII).

In Sec. VII we discuss a similar simulation in the real case, i.e., under real conditions, without the ideal $N_0 \to \infty$ assumption, along with a numerical proof of principle.

B. $\mathbb{Z}_N$ plaquettes

The effective construction of the $\mathbb{Z}_N$ Hamiltonian out of the fundamental Hamiltonian (55) in the loop method is similar to the derivation in the cQED case. The analogy applies to the ideal limit of the cQED simulation, as the interactions here are exactly unitary (i.e., the link operators are unitary). As before, one sets λ to be the largest energy scale, comparing to μ and ϵ. Initially, all the vertices are filled with bosons, as explained in the previous subsections.

In the first order we obtain H_E. In the second order we obtain an ignorable constant, thanks to the unitarity of the elementary interactions.

In the third order, as in the U(1) case, one obtains from the anticommutator contribution (see Sec. VI A) $-\frac{4\alpha\epsilon^2}{(2\lambda)^2}\mathcal{N}H_E$ (where $\mathcal{N}$ is the number of links, and $\alpha = -\mu/2$). From the other contribution, one obtains for each link

$$\frac{2\alpha\epsilon^2}{(2\lambda)^2}[2H_E + (QPQ^{\dagger} + QP^{\dagger}Q^{\dagger} + Q^{\dagger}PQ + Q^{\dagger}P^{\dagger}Q)], \tag{78}$$

where the 2 comes from the bosonic creation and annihilation operators of the vertices. The $\mathcal{N}H_E$-dependent terms from both contributions cancel. Using $QPQ^{\dagger} = e^{i\delta}P, QP^{\dagger}Q^{\dagger} = e^{-i\delta}P^{\dagger}$ ($\delta = \frac{2\pi}{N}$, see Sec. II B2) we get a renormalization to H_E

$$\delta^{(3)}H_E = \frac{\epsilon^2\mu}{\lambda^2}\sin^2\left(\frac{\delta}{2}\right)\sum_l(P_l + P_l^{\dagger}). \tag{79}$$

In the fourth order, the nonconstant contributions are two.

(i) An undesired term (which is still gauge invariant, of course)

$$H'_E = \frac{\epsilon^2\mu^2}{2\lambda^3}\cos(\delta)\sin^2\left(\frac{\delta}{2}\right)\sum_l\left(P_l^2 + P_l^{\dagger 2}\right). \tag{80}$$

This term becomes good $N = 2,3$, since for $N = 2$, $P^2 = P^{\dagger 2} = 1$ (and thus it is a constant), and for $N = 3$, $P^2 = P^{\dagger}$ and $P^{\dagger 2} = P$ and thus it is yet another renormalization of H_E.

(ii) The anticipated plaquette terms

$$H_B = -\frac{4\epsilon^4}{\lambda^3}\sum_{\mathbf{n}}(Q_{\mathbf{n},1}Q_{\mathbf{n}+\hat{\mathbf{1}},2}Q^{\dagger}_{\mathbf{n}+\hat{\mathbf{2}},1}Q^{\dagger}_{\mathbf{n},2} + \mathrm{H.c.}) \tag{81}$$

.

Thus, eventually, if we define a renormalized $\mu_{\mathrm{ren}} = \mu(1 - \frac{2\epsilon^2}{\lambda^2}\sin^2(\frac{\delta}{2}))$ and the appropriate $H_{E,\mathrm{ren}} = H_E + \delta^{(3)}H_E$, we obtain to fourth order the desired $\mathbb{Z}_N$ lattice gauge theory Hamiltonian, with some corrections

$$H_{\mathrm{eff}} = H_{E,\mathrm{ren}} + H_B + H'_E, \tag{82}$$

where for $N \to \infty$, $H_{E,\mathrm{ren}} \to H_E$ and $H'_E \to 0$, for $N = 2$ H'_E is an ignorable constant, and for $N = 3$ H'_E is another renormalization of into H_E, and thus in these two cases the simulation is exact.

C. SU(N) plaquettes

Finally, we shall describe the effective construction of an SU(N) gauge theory, using the appropriate elementary interactions (for the ideal case, in which they really contain unitary matrices), with the loop method. Again, for simplicity, we describe the $2+1$ dimensional case. We start with the Hamiltonian

$$H = H_E + H_{\text{int}} + H_C, \tag{83}$$

where the electric Hamiltonian of an SU(N) LGT as in Eq. (6) [again, we define $\mu = \frac{g^2}{2}$] and H_{int} is the appropriate elementary interaction (4), with some fixed representation r of the group. We choose it to be the fundamental representation, and for simplicity we shall next drop the representation index r when referring to the fundamental representation.

The spinors will be in the size of the representation, thus, for the fundamental representation of SU(N) we need N fermionic species. Besides interacting with the links in H_{int}, they are also constrained by H_C, which is similar to the previous constraining Hamiltonians. One such constraining Hamiltonian is

$$H_C = -\lambda \sum_{v \text{ special}} \psi_v^\dagger \psi_v = -\lambda \sum_{v \text{ special},a} \psi_{v,a}^\dagger \psi_{v,a}, \tag{84}$$

where we define the special vertices to be the ones with both indices even, i.e., it is energetically favorable for the fermions to be in special vertices. As before, we introduce another set of fermions, χ, with similar H_{int}, H_c constraining to other special vertices, with both the indices odd, and no interactions with the ψs. Each plaquette contains exactly two such vertices, one of each type (even or odd).

Initially, we prepare the system in one of two possible classes—either a pure state of the form

$$|\text{sys}\rangle = |\Psi\rangle \otimes |\{U\}\rangle, \tag{85}$$

where $|\{U\}\rangle$ is a bosonic state and $|\Psi\rangle$ is the state of the fermions, in which the "non-special" vertices contain no fermions at all, while the "special" ones are fully occupied, or the mixed state

$$\rho_{\text{sys}} = \rho_\Psi \otimes |\{U\}\rangle\langle\{U\}|, \tag{86}$$

where $|\{U\}\rangle\langle\{U\}|$ is the density matrix of some pure state of the bosons, and ρ_Ψ is a mixed state, in which the "non-special" vertices contain no fermions at all, while the "special" ones are each prepared in

$$\rho = \frac{1}{N}\sum_a |a\rangle\langle a|, \tag{87}$$

(where $|a\rangle$ corresponds to a state of a single a fermion, ψ or χ, depending on the site). In both the possibilities the initial state should be gauge invariant, of course.

As before, we set λ to be the largest energy scale in the Hamiltonian, and construct an effective Hamiltonian for its ground sector $\mathcal{M}_0$. In the case where the fermions are prepared in a mixed state, their "tracing out" will literally be tracing out, i.e. the effective Hamiltonian will be the result of a partial trace over the fermionic degrees of freedom, of the perturbative expansion, $\text{Tr}_{\text{F}}(H_{\text{eff}}\,\rho_\Psi)$.

1. *Effective nonplaquette terms*

In the first order, we obtain H_E. Then we are left with an effective Hamiltonian, acting on the pure state of bosons. In the second order, we get once again an ignorable constant, due the unitarity of the interactions.

We give here the derivation of terms of the initial mixed-state case, however, the final results of the initial pure-state case are very similar. Thus, we shall introduce for the final results the symbol ξ_{in}, which equals 1 if the initial state is pure, and $1/N$ if it is mixed.

The third-order terms are $H_{\text{eff}}^{(3)} = \mathcal{P}_0 H_1 \mathcal{K} H_1 \mathcal{K} H_1 \mathcal{P}_0 - \frac{1}{2}\{\mathcal{P}_0 H_1 \mathcal{K}^2 H_1 \mathcal{P}_0, \mathcal{P}_0 H_1 \mathcal{P}_0\}$. Let us examine the first part. Consider a special vertex 1, some link emanating from it (in the following example, negative) and the vertex on its other edge 2. We act with the terms constructed out of these components on a an element of a state in $\mathcal{M}_0$

$$\frac{\epsilon^2}{\lambda^2} \sum_{a,b,c,d,e,f} (\psi_1^\dagger)_a (U^\dagger)_{ab} (\psi_2)_b |0_1 e_2\rangle\langle 0_1 e_2| H_E |0_1 f_2\rangle \times \langle 0_1 f_2| (\psi_2^\dagger)_c U_{cd} (\psi_1)_d |d_1 0_2\rangle\langle d_1 0_2|. \tag{88}$$

H_E does not involve any fermions, and thus $\langle 0_1 e_2| H_E |0_1 f_2\rangle = \delta_{ef} H_E$. From the fermionic terms we get

$$(\psi_1^\dagger)_a (\psi_2)_b |0_1 e_2\rangle\langle 0_1 e_2| (\psi_2^\dagger)_c (\psi_1)_d |d_1 0_2\rangle\langle d_1 0_2| = \delta_{be}\delta_{ec} |a_1 0_2\rangle\langle d_1 0_2|. \tag{89}$$

Considering the entire local fermionic ensemble, and tracing it out, we get $\frac{1}{N}\delta_{bc}\delta_{ad}$, and eventually the contribution for each negative link $\frac{\epsilon^2}{N\lambda^2} U_{ab}^\dagger H_E U_{ba}$, and similarly, for a positive one, $\frac{\epsilon^2}{N\lambda^2}\sum_{ab} U_{ab} H_E U_{ba}^\dagger$.

$$U_{ab}^\dagger H_E U_{ba} = U_{ab}^\dagger (H_E - \mu \mathbf{E}^2) U_{ba} + \mu U_{ab}^\dagger \mathbf{E}^2 U_{ba} = \delta_{aa}(H_E - \mu \mathbf{E}^2) + \mu U_{ab}^\dagger \mathbf{E}^2 U_{ba}, \tag{90}$$

where $\mathbf{E}^2$ is the Casimir operator of the relevant link. Using the commutation relations of group elements with group generators (see Sec. II B 3), we get

$$\sum_{ab} (\delta_{aa}(H_E - \mu \mathbf{E}^2) + \mu U_{ab}^\dagger \mathbf{E}^2 U_{ba}) = \mu \text{Tr}(\lambda^2) + N H_E + \mu \sum_a \{E_a, \text{Tr}(T_a)\}, \tag{91}$$

where T_a is the matrix representation of E_a within the chosen representation, which for SU(N) is traceless.

For positive links, the only difference will be a change of sign to the last term, which is zero, so their contribution is the same. Altogether we get, neglecting the constant terms of $\text{Tr}(\lambda^2)$, $4\mathcal{N}_V \frac{\epsilon^2}{\lambda^2} H_E$, where $\mathcal{N}_V$ is the number of special even vertices (the 4 factor is due to the fact, that in two spatial dimensions, there are four links neighboring each vertex).

The other third-order contribution is of the form $-4\mathcal{N}_V \frac{\epsilon^2}{\lambda^2} H_E$, and thus the entire third-order contribution (neglecting ignorable constants) is zero. This is all thanks to the tracelessness of the matrix representations of SU(N)'s generators. Suppose we extended our gauge group to U(N); then we would have generators with nonzero trace, which

would lead to the Gauss's law terms and renormalizations, as in the U(1) case. The χ fermions will give rise, of course, to a similar contribution.

The fourth-order terms involving double operation of H_E, will similarly result in constants and canceled terms, thanks to the tracelessness of SU(N) generators. However, here we have one nonzero contribution, which is a renormalization to the electric part,

$$\delta H_E = -\frac{4\xi_{in}\mu^2\epsilon^2}{\lambda^3} C(r) \sum_{\mathbf{n},k,a} (E_{\mathbf{n},k})_a (E_{\mathbf{n},k})_a, \tag{92}$$

where for the fundamental representation of SU(N), $C(N) = 1/2$. Fourth-order contributions which go back and forth with $H_{\rm int}$ on two links give rise to constants as well, due to the unitarity.

2. The plaquette terms

Finally, we shall construct the plaquette interactions, which come, as in the U(1) case, from transferring auxiliary fermions around a plaquette. Here, after eliminating the fermionic degrees of freedom in the nonspecial vertices, one effectively gets, for example, terms such as

$$-\frac{\epsilon^4}{\lambda^3} \sum_{abcde} (\psi_v^\dagger)_a (U_1)_{ab} (U_2)_{bc} (U_3^\dagger)_{cd} (U_4^\dagger)_{de} (\psi_v)_e |e\rangle\langle e| \tag{93}$$

(with the conventions of Fig. 3, with v the vertex labeled there by $\mathbf{n}$). By tracing out the fermions, we get δ_{ae}, which closes the plaquette and introduces the desired group trace. This yields the plaquette Hamiltonian

$$H_B = -\frac{2\xi_{in}\epsilon^4}{\lambda^3} \sum_{\text{plaquettes}} [\mathrm{Tr}(U_1 U_2 U_3^\dagger U_4^\dagger) + \text{H.c.}] \tag{94}$$

(the factor 2 is due to the two types of auxiliary fermions) and eventually we get effectively, up to fourth order, the SU(N) pure-gauge Kogut-Susskind Hamiltonian,

$$H_{\rm eff} = H_E + \delta H_E + H_B \tag{95}$$

without any corrections (δH_E is just a renormalization). Moreover, the leading order of ϵ is the fourth one, and thus here it is even sufficient to demand $\epsilon^4 \ll \lambda^4$.

One should also note that by introducing other set of fermions, interacting with the bosons with a similar $H_{\rm int}$ but nonconstrained, one can introduce dynamic fermions to the system. This is discussed in Sec. VIII.

VII. QUANTUM SIMULATION OF 2 + 1-D GAUGE THEORIES

Putting together the elementary link interactions of Sec. IV, and the loop method for the plaquette interactions of Sec. VI, one could construct quantum simulations of lattice gauge theories in 2 + 1 dimensions. However, in several cases one would have to face real conditions, instead of the ideal conditions of the previous section, such as the use of finite Hilbert spaces instead of infinite ones. In that sense, the quantum simulation of $\mathbb{Z}_N$ is the most accurate: in this theory, the local Hilbert spaces are already of finite dimension, and thus nothing should be added to the discussion of these models in the previous section.

On the other hand, quantum simulation of the continuous gauge theories—U(1) and SU(N)—require some truncation of the Hilbert space (this was already mentioned in the case of the Schwinger model, in Sec. V A). In the case of cQED, the simulation requires the use of BECs. In this section we show that it should still work with a finite number of bosons per link, derive the conditions for that, and give numerical evidence. Finally we shall comment on the SU(2) 2 + 1-d simulation.

A. 2 + 1-d simulation of cQED using a finite number of bosons

We have shown in Sec. VI A how to obtain, effectively, the plaquette interactions using the already gauge invariant elementary interactions. However, in the derivation we have used unitary matrices in the elementary interactions ($N_0 \to \infty$), whereas in the real scenario $N_0 = 2\ell$ is finite, even if it is large, and thus the interactions contain angular momentum ladder operators (38), which are nonunitary. Here we shall describe how to handle these effects in order to achieve an accurate simulation despite the nonunitarity.

We still include the χ fermions, with the same constraining part (71), but now $H_{\rm int}$ takes the form

$$H_{\rm int} = \frac{\epsilon}{\sqrt{\ell(\ell+1)}} \sum_{\mathbf{n},k} (\psi_{\mathbf{n}}^\dagger L_{+,\mathbf{n},k} \psi_{\mathbf{n}+\hat{\mathbf{k}}} + \chi_{\mathbf{n}}^\dagger L_{+,\mathbf{n},k} \chi_{\mathbf{n}+\hat{\mathbf{k}}} + \text{H.c.}). \tag{96}$$

1. First- and second-order contributions

In the first order, we get H_E as before. In the second order, we get the same type of contributions, but now they will not be constant anymore. What we have now are contributions of the form

$$-\frac{\epsilon^2}{\lambda} \frac{L_\pm L_\mp}{\ell(\ell+1)} = -\frac{\epsilon^2}{\lambda} \left(1 - \frac{L_z^2}{\ell(\ell+1)} \pm \frac{L_z}{\ell(\ell+1)}\right) \tag{97}$$

(where $L_+ L_-$ is for positive links, and vice versa for the negative ones). This contribution becomes constant as $\ell \to \infty$, because then, any eigenvalue of L_z satisfies $m \ll \ell$. In the case of a finite ℓ, one can neglect the first constant, and after summing on all the links, obtain a renormalization factor for the electric Hamiltonian from the L_z^2 term, and a Gauss's law (which is an ignorable constant) from the linear L_z part, which has the correct signs. Thus, second order leads to a renormalization of H_E (and this is why the χs are important).

2. Third- and fourth-order contributions

Here, after canceling the equal part in the two possible contributions (see the previous section), we are left with

$$\frac{\mu\epsilon^2}{\lambda^2} (1 \mp 2L_z) \frac{L_\pm L_\mp}{\ell(\ell+1)}, \tag{98}$$

where the choices of signs for positive/negative links are as in the second order.

Again, in the ideal limit, $\frac{L_\pm L_\mp}{\ell(\ell+1)} \underset{\ell\to\infty}{\longrightarrow} 1$, and then we get a constant + Gauss's laws (which are constants too). However, for a finite ℓ, the contributions are again nonconstant: besides

the constants, we get linear terms in L_z, which correspond to Gauss's law, and a third-order renormalization of H_E, but also L_z^3 terms. If we work with $\ell = N_0/2 = 1$, $L_z^3 = L_z$ and thanks to the correct signs get Gauss's law again. However, this is not a very interesting and obviously not the general case, and thus we wish to find some way to deal with these extra terms. We shall first focus on the fourth-order contributions, and then conclude what to do about the problematic terms from both orders.

In the fourth order there are three types of contributions. First, the plaquette terms, which now take the form

$$H_B = -\frac{2\epsilon^4}{\lambda^3 \ell^2(\ell+1)^2} \times \sum_{\mathbf{n}} (L_{+,\mathbf{n},1} L_{+,\mathbf{n}+\hat{\mathbf{1}},2} L_{-,\mathbf{n}+\hat{\mathbf{2}},1} L_{-\mathbf{n},2} + \text{H.c.}). \quad (99)$$

The second type of terms involve operations with H_{int} only, and they include, after the reduction of constants, products of L_z and L_z^2 of neighboring links intersecting in odd vertices. This term is in the same order of the plaquette terms, $O(\frac{\epsilon^4}{\lambda^3})$. These terms, which we call H_B', are indeed unwanted terms, but can still be tolerated as they are gauge invariant and not stronger than the plaquette interactions.

The third terms take the form $-\frac{\epsilon^2\mu^2}{\lambda^3\ell(\ell+1)}\{L_z, L_\pm\}\{L_z, L_\mp\}$ on positive/negative links. These terms will renormalize H_E in the ideal limit, but for a finite ℓ will include, besides the constants, L_z and L_z^2 terms, which are treatable, also L_z^3 and L_z^4 terms (again, with the correct signs to contribute to Gauss's law and renormalize H_E for $\ell = 1$). In order to eliminate the effect of these terms, along with the undesired third-order terms, we define $\mu \equiv \beta\frac{\epsilon^2}{\lambda}$, where $\beta \leqslant 1$ is a dimensionless parameter. Then, the undesired third-order terms are $O(\frac{\epsilon^4}{\lambda^3})$, like the plaquettes, and thus can be tolerated, at least for states which are superpositions of $m \ll \ell$ mostly. The fourth-order undesired terms become effectively sixth-order terms, $O(\frac{\epsilon^6}{\lambda^5})$, and thus can be safely neglected.

Thus, for a finite $N_0 = 2\ell$, if the parameters are tuned correctly one gets, effectively up to constant, the Hamiltonian

$$H_\ell = \tilde{H}_E + H_B + O\left(\frac{\epsilon^4}{\lambda^3}\right) \quad (100)$$

with

$$\tilde{H}_E = \left(\frac{\beta}{\lambda} + \frac{1}{\ell(\ell+1)}\right)\frac{\epsilon^2}{\lambda}\sum_{\mathbf{n},k}(E_{\mathbf{n},k})^2, \quad (101)$$

which is expected to give rise to the same dynamics as the Kogut-Susskind Hamiltonian $H = \tilde{H}_E + H_B$, at least for a regime in which $\frac{\epsilon^4}{\lambda^3}$ is small enough, i.e., not in the extreme weak limit, but apparently not only in the strong limit, but also in a regime where H_E, H_B are of the same order of magnitude. The two Hamiltonians have to differ by a constant, at least for states which are superpositions mostly of $m \ll \ell$.

In order to see that, we shall consider some numerical results. But before that, let us point out two important issues about the Hamiltonian parameters. Although the relation $\mu \equiv \beta\frac{\epsilon^2}{\lambda}$ might seem to imply that H_E will always be stronger than H_B, because of the powers of ϵ and λ, one should note that thanks to β, which can be chosen small, one can still go to weaker regimes. Moreover, as in the ideal case, H_{int} only contributes to the effective Hamiltonian in even repetitions, and thus, again, it is sufficient to demand $\epsilon^2 \ll \lambda^2$ rather than $\epsilon \ll \lambda$.

B. 2 + 1-d cQED simulation: A numerical proof of principle

In order to see whether the real case simulation still yields valuable results, one has to check the effects of the $O(\frac{\epsilon^4}{\lambda^3})$ in H_ℓ (100). This can be done if one compares the spectrum of the desired Hamiltonian,

$$\tilde{H}_\ell = \tilde{H}_E + H_B \quad (102)$$

with the spectrum of the lower-energy sector (i.e., the states fulfilling the constraint) of the fundamental Hamiltonian,

$$H = H_E + H_{\text{int}} + H_C. \quad (103)$$

The accuracy of the simulation will be deduced from the observation of a constant energy shift between the spectra of the two Hamiltonians. This will mean that both of them give rise to the same dynamics. Such results will trivially take place in the strong coupling limit, where $\epsilon \to 0$. However we wish to check what happens in other coupling regimes.

We have run numerical simulations of a single plaquette, using the parameters $\lambda = 10, \epsilon = 0.1$. We changed the values of ℓ, β, using the convenient dimensionless ratio between the scales of H_E and H_B,

$$x = \frac{1}{2}\left(\frac{\beta}{\lambda} + \frac{1}{\ell(\ell+1)}\right)\frac{\lambda^2}{\epsilon^2} \quad (104)$$

parametrizing the coupling strength. We have chosen the subspace with no (real) static charges.

We have calculated the spectra $\{E\}$ of H's ground sector, as well as $\{\tilde{E}\}$ of $\tilde{H}$ for several values of ℓ and x and calculated the value of

$$d \equiv \left|\frac{\text{std}(E-\tilde{E})}{\text{mean}(E-\tilde{E})}\right|. \quad (105)$$

As one can see in Fig. 14, this value is fairly small, getting larger, as anticipated, for smaller values of the simulation parameters. However, on the other hand, if one wishes to evaluate the quality of simulations, it should be noted that in order to get an accurate simulation (compared to the original Kogut-Susskind model) in the weak coupling limit (small x) one has to pick a sufficiently large value of ℓ [13]. If only the ground state is of interest, lower ℓ are possible. In order to achieve a better accuracy for excited states, one must increase ℓ. This can be seen in Fig. 15.

Furthermore, as x gets smaller, the energy scales of the two Hamiltonians $H, \tilde{H}$ separate (as can be seen in Fig. 15). Thus, the difference between them can still be treated approximately as a constant, due to the difference of scales, but yet one should note this qualitative subtlety as well, treating the left region of Fig. 14 more carefully. On the other hand, for $x \gtrsim 1$, using sufficiently large ℓs, which tend to get smaller as x is increased (see Fig. 16), the scales of two Hamiltonians correspond and the d value is credible. As one can conclude from that, a simulation which is accurate both comparing to

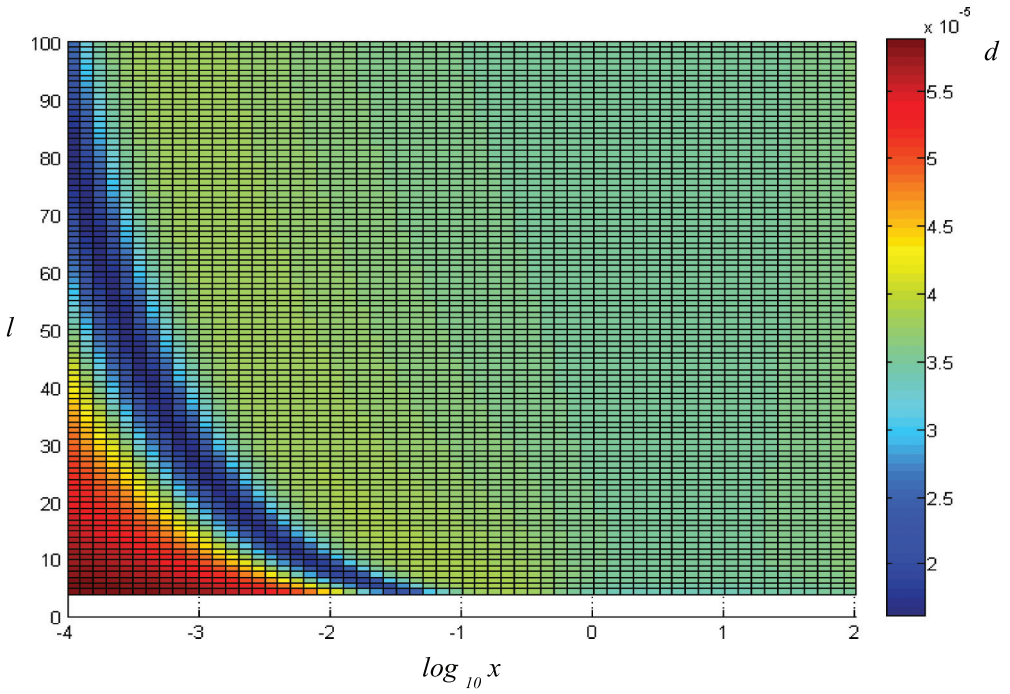

FIG. 14. (Color online) A plot of d [Eq. (105)] for several values of ℓ,x. One can see that d grows as ℓ,x decrease. However, in this very same region of parameters, the credibility of it is low, as explained in the text.

the Kogut-Susskind model and with fairly constant effective Hamiltonian contributions is possible for $x \gtrsim 1$.

C. 2 + 1-d SU(N) Yang-Mills simulation

In the case of non-Abelian theories, such as SU(2), relying on Ref. [17] for the elementary interactions (as described in Sec. IV C), one could simulate a version of SU(2) gauge theory in which the bosonic operators in the elementary interactions are not unitary (63).

In the 1 + 1-d case we could establish a good approximation for the unitary interactions, since the elementary interactions only change N by ± 1, or j by $\pm 1/2$ on single links. However, here, since there are plaquette interactions, we have such processes on four links at once. One can also introduce dynamic fermions, and altogether we lose the fifth-order accuracy we had in the 1 + 1-d case. Moreover, the effective Hamiltonian series may include, in this case, more terms (as we had in the real cQED case comparing to the ideal unitary case). This will depend on these N as well. On the other hand, note that all these corrections are nevertheless gauge invariant; gauge invariance is not ruined.

Therefore we conclude that due to the $\sqrt{N+1}$ operators, which would lead, already in first order in $H_{\text{int}}^{\text{eff}}$ (63), to terms with different amplitudes than in regular SU(2) theory, the [17] realization of SU(2) elementary interactions allows only for simulation of SU(2) gauge theories near the strong coupling limit. However, in this regime, it should reproduce the same physics, qualitatively.

VIII. INCLUSION OF DYNAMICAL FERMIONS

We have presented methods to construct 1 + 1 dimensional simulations of continuous gauge theories [U(1), SU(N)] with dynamic matter, and have shown how, by extending to more spatial dimensions and replacing the mass Hamiltonian H_M with the appropriate constraint, H_C, one can use the fermions as auxiliary particles to construct effective plaquette interactions.

Here we shall discuss the ability to introduce dynamical fermions for these theories as well. All one has to do, is to include on top of the auxiliary fermions ψ and χ, more fermionic species Ψ. These occupy the vertices as well, and the number of species should be chosen according to the group, for example, one per vertex for U(1), N per vertex for SU(N).

The fermionic dynamics are described by the Dirac Hamiltonian H_D, which is of course gauge invariant and consists of local mass terms [H_M, see Eq. (2)] and elementary interactions in the form of H_{int} (4). Of course, the system must be prepared such that there will not be any direct Ψ-ψ and Ψ-χ interactions.

For a U(1) theory in 2 + 1 dimensions, for example, one should pick

$$H_D = M\sum_{\mathbf{n}}(-1)^{n_1+n_2}\Psi_{\mathbf{n}}^{\dagger}\Psi_{\mathbf{n}} + \gamma\sum_{\mathbf{n},k}(\Psi_{\mathbf{n}}^{\dagger}e^{i\phi_{\mathbf{n},k}}\Psi_{\mathbf{n}+\hat{\mathbf{k}}} + \Psi_{\mathbf{n}+\hat{\mathbf{k}}}^{\dagger}e^{-i\phi_{\mathbf{n},k}}\Psi_{\mathbf{n}}). \quad (106)$$

The dynamic fermions (Ψ) are not constrained and thus H_D appears in the first order of the effective Hamiltonian, and makes no contribution to the second one.

In the third and fourth order one has to be more cautious. First, suppose that the elementary interactions contain unitary

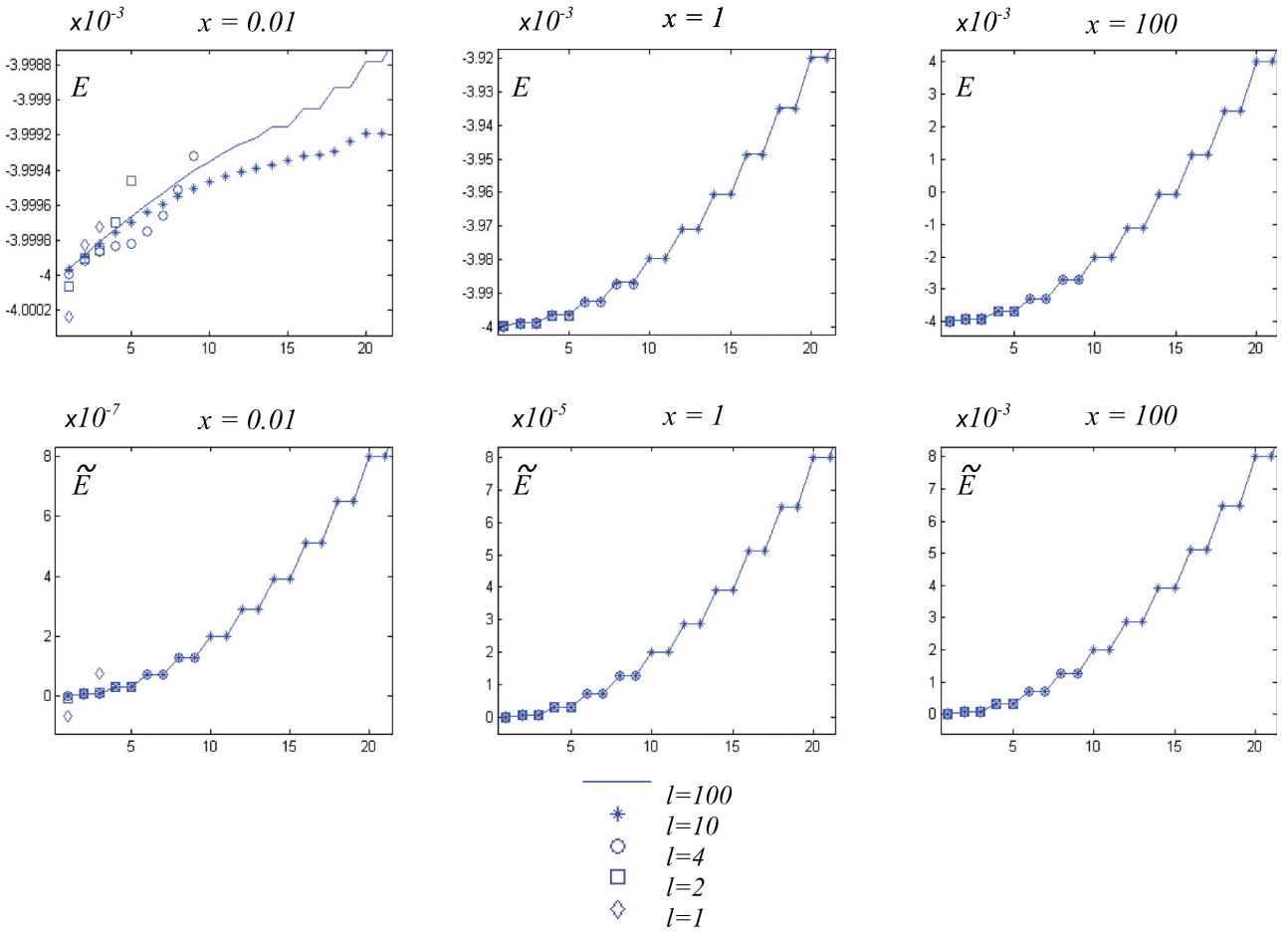

FIG. 15. (Color online) Plots of the spectra of H (upper panel) and $\tilde{H}$ (lower panel) for small values of ℓ and several values of x, compared to the fairly reasonable approximation of the nontruncated Kogut-Susskind model using $\ell = 100$. Note that the qualitative correspondence of the two spectra arises as x, ℓ increase.

operators (as in Sec. VI). There,

$$[H_D, H_{\text{int}}] = 0 \tag{107}$$

and thus H_D makes no contribution to the third and fourth orders (as well as to higher ones) and we get the desired results.

In case the interactions are not exactly unitary (as in the models of Sec. VII), there will be some nonvanishing contributions in higher orders. However, they will all be gauge invariant, and introduce only small corrections to the desired interactions. For example, in a U(1) (cQED) simulation with finite number of bosons (as in Sec. VII A), where H_D takes the form

$$H_D = M\sum_{\mathbf{n}}(-1)^{n_1+n_2}\Psi^\dagger_{\mathbf{n}}\Psi_{\mathbf{n}} + \frac{\gamma}{\sqrt{\ell(\ell+1)}} \times \sum_{\mathbf{n},k}(\Psi^\dagger_{\mathbf{n}}L_{+,\mathbf{n},k}\Psi_{\mathbf{n}+\hat{\mathbf{k}}} + \Psi^\dagger_{\mathbf{n}+\hat{\mathbf{k}}}L_{-,\mathbf{n},k}\Psi_{\mathbf{n}}) \tag{108}$$

one obtains third-order corrections of the form

$$\frac{\epsilon^2\gamma}{\lambda^2}\left(\Psi^\dagger_{\mathbf{n}}L_{+,\mathbf{n},k}\frac{L_{z,\mathbf{n},k}}{[\ell(\ell+1)]^{3/2}}\Psi_{\mathbf{n}+\hat{\mathbf{k}}} + \text{H.c.}\right) \tag{109}$$

for a positive link, and

$$-\frac{\epsilon^2\gamma}{\lambda^2}\left(\Psi^\dagger_{\mathbf{n}}\frac{L_{z,\mathbf{n},k}}{[\ell(\ell+1)]^{3/2}}L_{+,\mathbf{n},k}\Psi_{\mathbf{n}+\hat{\mathbf{k}}} + \text{H.c.}\right) \tag{110}$$

for a negative one. This is a negligible (third-order) correction to H_D, but is gauge invariant, of course.

Another consequence of introducing dynamic charges is that the divergence of electric field is no longer a constant of motion, it is now equal to the dynamic charge on the vertex, which is dynamic. The effective terms in the U(1) simulation include such divergences, which have been previously, for static charges, dismissed as constants in the Hamiltonian. Now this is not the case, and these terms should be taken into account. However, we only obtain this Gauss's Law contributions at special vertices (where the auxiliary fermions are constrained to be). This introduces an asymmetry to the system. Nevertheless, Gauss's law is still satisfied (as the symmetry is not broken), and thus the spectrum is still divided into sectors of static charges. If one initially prepares the system in a state where there are no static charges, only the dynamical ones contribute to Gauss's law and thus these local divergences of the electric field are proportional to the charge, which is expressed in terms of the local Ψ number in the special vertices. Thus one can introduce counterterms, proportional to $\Psi^\dagger\Psi$ on special vertices to eliminate this asymmetry. Note that these are merely corrections to the mass M in H_M in the special vertices.

For a completely unitary theory, these Gauss's law terms start to appear only in the third order (see Sec. VI A2) and thus

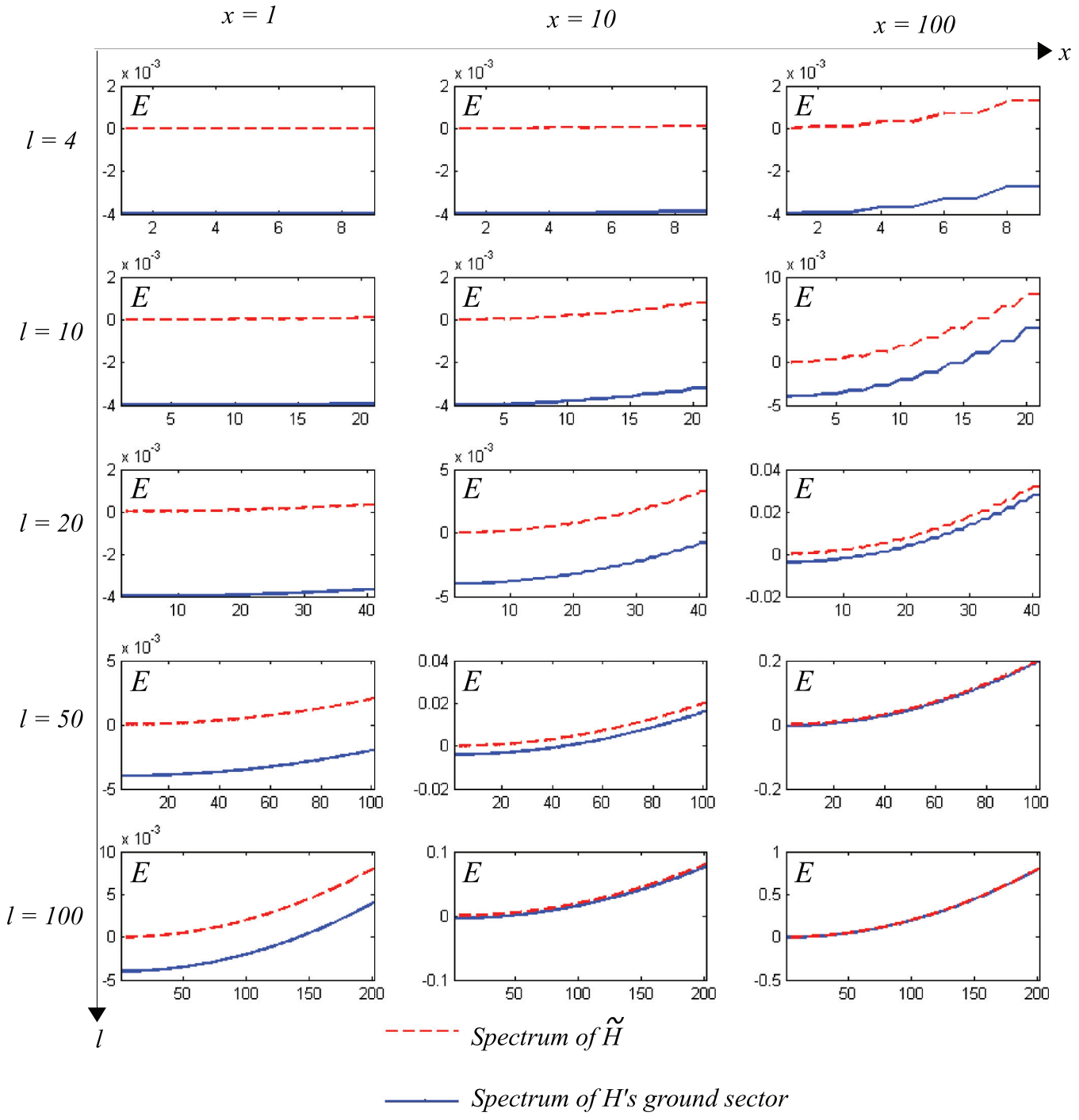

FIG. 16. (Color online) Plots of the spectra of $H, \tilde{H}$, enabling a qualitative impression on the constant difference between them, for several values of the simulation parameters x, ℓ.

the required counterterms are initially very weak and thus their contribution to the effective series may be taken into account only in the first order (where it is required). In a real theory with angular momentum operators, such Gauss's laws appear already in the second order (see Sec. VII A1), the counterterms have to be a little stronger and, in order to have the possibility to disregard their contributions to elements in the effective series in orders higher than 1, the interactions parameters must be chosen carefully.

IX. SUMMARY AND CONCLUSION

In this paper we have presented a method for the simulation of lattice gauge theories in high-energy physics, using ultracold atoms in optical lattices. Unlike previous proposals where the gauge invariance was obtained effectively, here the gauge invariance is fundamentally in the atomic Hamiltonian, without using perturbation theory. This is done by utilizing the conservation of hyperfine angular momentum, introducing the

gauge-invariant elementary matter–gauge-field interactions along links.

At a second stage, the nonlinear self-interactions of the gauge fields along plaquettes are constructed effectively, using the introduced loop method, from the already gauge-invariant Hamiltonian with the elementary interactions. Although the derivation uses fourth-order perturbation theory, it is effectively to second order, due to the vanishing of the relevant odd orders.

Among the simulation proposals in these paper was the suggestion to simulate compact QED in $1+1$ dimensions—the Schwinger model. This simulation scheme utilizes in this case a small number of atomic species and does not involve perturbative and effective methods at all. Thus it could serve as the first step toward the realization of quantum simulations of gauge theories and high-energy physics models.

ACKNOWLEDGMENTS

E.Z. is supported by the Adams Fellowship Program of the Israel Academy of Sciences and Humanities. I.C. is partially supported by the EU project AQUTE. B.R. acknowledges the support of the Israel Science Foundation, the German-Israeli Foundation, and the European Commission (PICC).

APPENDIX: FURTHER DETAILS ON THE LATTICE GAUGE THEORIES DISCUSSED IN THE PAPER

1. Confinement in cQED

In this section we briefly review confinement in cQED, whose Hamiltonian was discussed in Sec. II B 1. Let us consider first the states of the pure gauge theory, i.e., with no dynamical matter. In this case only static charges are possible, and the Hamiltonian is the Abelian Kogut-Susskind Hamiltonian (14). Suppose we use the local flux basis, i.e., the basis consisting of products of flux states over the links of the entire lattice. In the strong coupling limit, where $g^2 \to \infty$, this basis is a good choice, as its elements are eigenstates of H_E. Note, however, that these eigenstates are divided into several sectors, depending on the static charges—eigenvalues of $G_{\mathbf{n}}$, as these are constants of motion, setting the Gauss's law (13). Let us discuss this limit, taking H_B as a perturbation to H_E.

Consider, in the strong limit, the case of a single charge $Q_{\mathbf{n}} = 1$ in some vertex $\mathbf{n}$. In order to respect Gauss's law, an infinite string of flux must be introduced to the system. In fact, the (degenerate) zeroth-order ground state of this charge sector is already of infinite energy: an infinite string of flux ± 1 must emanate from $\mathbf{n}$. This is evidence of charge confinement in the strong limit: a single charge costs infinite energy. Thus we must consider bound states of at least two charges. Let us have a look at the state of two such charges, say $Q_{\mathbf{n}} = 1$ and $Q_{\mathbf{n}+R\hat{\mathbf{k}}} = -1$. There, the zeroth-order eigenstate consists of a string of flux 1, connecting the charges, i.e., the state

$$|R^{(0)}\rangle = \psi^\dagger_{\mathbf{n}} \prod_{i=0}^{R-1} e^{i\phi_{\mathbf{n}+i\hat{\mathbf{k}}}} \psi_{\mathbf{n}+R\hat{\mathbf{k}}} |\mathrm{vac}\rangle, \tag{A1}$$

where $\psi_{\mathbf{n}}$, $\psi^\dagger_{\mathbf{n}}$ create positive/negative static charges in the appropriate vertices and $|\mathrm{vac}\rangle$ is the zeroth-order chargeless ground state, with flux zero everywhere. Note that this state is gauge invariant [just check the Abelian version of the local gauge transformation laws (3), (5)]. This state describes an electric flux tube, as expected within a confining phase. The energy of such a state, to zeroth order, is just the eigenvalue of H_E

$$H_E |R^{(0)}\rangle = \frac{g^2}{2} R |R^{(0)}\rangle. \tag{A2}$$

The static energy of this particle-antiparticle bound pair (a meson) is proportional to R (up to higher-order corrections, $O(g^{-4})$. This manifests the linear potential law, expected in a confining phase: $V(R) \propto R$, unlike the well-known Coulomb phase behavior, $V(R) \propto R^{-1}$.

The weak limit $g^2 \to 0$, however, is different. There, H_B is stronger, and these flux states are no longer eigenstates of the system, even not approximate ones. In $3+1$ dimensions, there is a phase transition to a Coulomb phase [25]. In $2+1$ dimensions, the theory confines for all values of the coupling constant, and it is a nonperturbative effect [23,31–33]. This is also the case for $1+1$ dimensions, where the theory is exactly solvable. When temperature enters the game as well, there is a phase transition to a Coulomb phase for small g also in the case of $2+1$ dimensions [68,69].

One may wish, as we do here for simulation purposes, to consider the case of a finite, truncated, local Hilbert space. In this case, the strong limit behavior is unaffected. For the weak limit, only when it is confining one can approximate the behavior of the real theory, as in the confining phase only a few number of low flux states is needed. The approximation becomes better as the truncation value ℓ is stronger, but also for small values of ℓ a reasonable approximation holds [13]. This is true when one considers the lattice theory; in terms of the continuum limit, if the truncation is done properly one can regain the right continuum limit (see, for example, the link models [50–53]).

2. Dynamic fermions in cQED

Including dynamic fermions in a lattice gauge theory is a bit problematic, due to the doubling of fermions in the continuum limit. We focus in this paper, and thus here, in the method of staggered fermions [34]. There, the continuum spinors decompose into two neighboring vertices of the lattice, one containing particles and the other, antiparticles. Two-component continuum spinors (which are sufficient for $1+1$ dimensional theories, and also for $2+1$ dimensional ones, if one is not interested in the chiral anomaly) are thus formed of two neighboring vertices, containing up to a single fermion each. This is why the H_M part of the Hamiltonian (35) contains the masses with alternating signs: the odd vertices represent the antiparticles, and they are filled in the ground state, forming the Dirac sea. Moreover, the dynamic charge $Q_{\mathbf{n}}$, present in Gauss's law (7) is defined as

$$Q_{\mathbf{n}} = \psi^\dagger_{\mathbf{n}} \psi_{\mathbf{n}} - \tfrac{1}{2}[1 - (-1)^{n_1+n_2}] \tag{A3}$$

(for simplicity this is a $2+1$ dimensional definition, which can be generalized to other dimensions, keeping the vertices' parity properties). This is in agreement with the particle/antiparticle picture: even vertices, representing particles, can be occupied by no fermions, corresponding to no mass and no charge, or a single fermion, corresponding to a particle with mass M and

charge $+1$. Occupied odd vertices have no mass (relative to $-M$) and no charge, and correspond to vacant vertices in the HEP picture, while empty vertices have mass M (relative to $-M$) and charge -1, representing an antiparticle.

The fermionic interactions are obtained with the gauge invariant H_{int}, whose Abelian form is (15). However, one should note that in order to get the Dirac equation in the continuum limit, some phases should introduced to this Hamiltonian, and they can be achieved using canonical transformations (which are not required to be implemented experimentally) on the fermions. For example, in a $1+1$ dimensional system, one can use the transformation (cf. footnote 5). The phase prescription for $3+1$ dimensions, yielding four-component spinors, is given in Ref. [34].

3. Confinement in $\mathbb{Z}_N$ gauge theories

Confinement for these theories is especially interesting, as it was argued [70] that confinement of quarks in QCD [SU(3)] has to do with the group's center, which is the group $\mathbb{Z}_3$. Thus the phase structure of $\mathbb{Z}_N$ is interesting [35,71,72]. The theory confines in the strong coupling limit ($\mu \to \infty$). Both in $2+1$ and in $3+1$ dimensions it is not the only phase. In $3+1$ dimensions, due to the self-dual nature of the theory, there is a phase transition from electric confinement for large coupling to a magnetic confinement in the small coupling regime, for $N < N_C$ ($N_c \approx 6$). For $N > N_C$ there is a third phase, with no confinement at all. In $2+1$ dimensions there is a phase transition and the theory does not confine in the weak limit [35]. However, for $N \to \infty$ the theory shows the phase transition at $g = 0$ [72], in accordance with the single confining phase structure of U(1) (the $N \to \infty$ limit of $\mathbb{Z}_N$).

4. SU(N) gauge theories: Dynamic fermions and confinement

In order to introduce dynamical fermions, we choose to utilize the method of staggered fermions again. We choose, as usual, to suppress flavor and spin indices, and identify the spinor components only by group indices, as in Eq. (1). With staggered fermions the masses are positive/negative alternately, similarly to (35). This time, the non-Abelian charge is defined as

$$(Q_{\mathbf{n}})_a = \sum_{bc} (\psi^\dagger_{\mathbf{n}})_b (T_a)_{bc} (\psi_{\mathbf{n}})_c = \frac{1}{2} \sum_{bc} (\psi^\dagger_{\mathbf{n}})_b (\sigma_a)_{bc} (\psi_{\mathbf{n}})_c \tag{A4}$$

(where the second equality holds for the fundamental representation). This is a fermionic Schwinger representation, and thus a full vertex has a zero charge. Thus one can establish a Dirac sea, similarly the Abelian one (Appendix A1), where vacancies in odd vertices correspond to antiparticles, measuring the masses there relative to $-M$ per fermion.

One can also consider static charges (i.e., with infinite mass). In particular, one would like to examine the confinement of static fundamental charges. This was initially done by Wilson [22] and later other authors in the Euclidean approach [23,31], but we shall concentrate on the Hamiltonian picture. Consider the strong limit of the theory, $g^2 \gg 1$, in which the electric part is much stronger than the magnetic part, which may be thus considered as a perturbation (as in the Abelian case). In this context, the ground state of two charges in $\mathbf{n}, \mathbf{n} + R\hat{\mathbf{x}}$, is the non-Abelian analog to (A1): Thus, the links along the straight line connecting the charges are excited to $j = \frac{1}{2}$, contributing zeroth-order energy $\frac{g^2}{2} j(j+1) = \frac{3}{4}\frac{g^2}{2}$, while the other links are in the singlet $j = 0$, contributing no energy at all in zeroth order. Therefore the energy of this state, to zeroth order, is $E(\phi) = \frac{3}{4}\frac{g^2}{2} R$ (as there are R excited links), and we get confining behavior, $V(R) \propto R$ again: the static energy (potential) between two static quarks is proportional to their distance. The string tension, E/R, is $\frac{3}{4}\frac{g^2}{2}$ in this case [26]. Other coupling regimes will not be treated here. We shall only comment that as the coupling decreases within a confining phase, the flux tube broadens and $|\phi\rangle$ is no longer an eigenstate of the Hamiltonian, in accordance with the growth of perturbative corrections, until the breakdown of perturbation theory.

[1] R. Feynman, Int. J. Theor. Phys. **21**, 467 (1982).
[2] M. Lewenstein, A. Sanpera, and V. Ahufinger, *Ultracold Atoms in Optical Lattices: Simulating Quantum Many-body Systems* (Oxford University Press, Oxford, 2012).
[3] I. Bloch, J. Dalibard, and S. Nascimbene, Nature Phys. **8**, 267 (2012).
[4] R. Blatt and C. F. Roos, Nature Phys. **8**, 277 (2012).
[5] J. I. Cirac and P. Zoller, Nature Phys. **8**, 264 (2012).
[6] J. I. Cirac, P. Maraner, and J. K. Pachos, Phys. Rev. Lett. **105**, 190403 (2010).
[7] A. Bermudez, L. Mazza, M. Rizzi, N. Goldman, M. Lewenstein, and M. A. Martin-Delgado, Phys. Rev. Lett. **105**, 190404 (2010).
[8] O. Boada, A. Celi, J. I. Latorre, and M. Lewenstein, New J. Phys. **13**, 035002 (2011).
[9] E. Kapit and E. Mueller, Phys. Rev. A **83**, 033625 (2011).
[10] E. Zohar and B. Reznik, Phys. Rev. Lett. **107**, 275301 (2011).
[11] L. Mazza, A. Bermudez, N. Goldman, M. Rizzi, M. A. Martin-Delgado, and M. Lewenstein, New J. Phys. **14**, 015007 (2012).
[12] O. Boada, A. Celi, J. I. Latorre, and M. Lewenstein, Phys. Rev. Lett. **108**, 133001 (2012).
[13] E. Zohar, J. I. Cirac, and B. Reznik, Phys. Rev. Lett. **109**, 125302 (2012).
[14] D. Banerjee, M. Dalmonte, M. Müller, E. Rico, P. Stebler, U.-J. Wiese, and P. Zoller, Phys. Rev. Lett. **109**, 175302 (2012).
[15] E. Zohar, J. I. Cirac, and B. Reznik, Phys. Rev. Lett. **110**, 055302 (2013).
[16] L. Tagliacozzo, A. Celi, A. Zamora, and M. Lewenstein, Ann. Phys. (NY) **330**, 160 (2013).
[17] E. Zohar, J. I. Cirac, and B. Reznik, Phys. Rev. Lett. **110**, 125304 (2013).
[18] D. Banerjee, M. Bgli, M. Dalmonte, E. Rico, P. Stebler, U.-J. Wiese, and P. Zoller, Phys. Rev. Lett. **110**, 125303 (2013).
[19] L. Tagliacozzo, A. Celi, P. Orland, and M. Lewenstein, arXiv:1211.2704 [cond-mat.quant-gas].
[20] E. Zohar and B. Reznik, New J. Phys. **15**, 043041 (2013).
[21] C. N. Yang and R. L. Mills, Phys. Rev. **96**, 191 (1954).
[22] K. G. Wilson, Phys. Rev. D **10**, 2445 (1974).

[23] A. M. Polyakov, Nucl. Phys. B **120**, 429 (1977).
[24] J. Kogut and L. Susskind, Phys. Rev. D **11**, 395 (1975).
[25] J. B. Kogut, Rev. Mod. Phys. **51**, 659 (1979).
[26] J. B. Kogut, Rev. Mod. Phys. **55**, 775 (1983).
[27] M. Troyer and U.-J. Wiese, Phys. Rev. Lett. **94**, 170201 (2005).
[28] D. H. Rischke, Prog. Part. Nucl. Phys. **52**, 197 (2004).
[29] M. G. Alford, A. Schmitt, K. Rajagopal, and T. Schäfer, Rev. Mod. Phys. **80**, 1455 (2008).
[30] K. Fukushima and T. Hatsuda, Rep. Prog. Phys. **74**, 014001 (2011).
[31] T. Banks, R. Myerson, and J. Kogut, Nucl. Phys. B **129**, 493 (1977).
[32] S. D. Drell, H. R. Quinn, B. Svetitsky, and M. Weinstein, Phys. Rev. D **19**, 619 (1979).
[33] S. Ben-Menahem, Phys. Rev. D **20**, 1923 (1979).
[34] L. Susskind, Phys. Rev. D **16**, 3031 (1977).
[35] D. Horn, M. Weinstein, and S. Yankielowicz, Phys. Rev. D **19**, 3715 (1979).
[36] C. E. Soliverez, J. Phys. C: Solid State Phys. **2**, 2161 (1969).
[37] C. Cohen-Tannoudji, G. Grynberg, and J. Dupont-Roc, *Atom-Photon Interactions: Basic Processes and Applications* (Wiley, New York, 1992).
[38] T. Banks, L. Susskind, and J. Kogut, Phys. Rev. D **13**, 1043 (1976).
[39] G. 't Hooft, Nucl. Phys. B **75**, 461 (1974).
[40] C. G. Callan, N. Coote, and D. J. Gross, Phys. Rev. D **13**, 1649 (1976).
[41] E. Witten, Commun. Math. Phys. **92**, 455 (1984).
[42] Y. Frishman and J. Sonnenschein, Phys. Rep. **223**, 309 (1993).
[43] K. Hornbostel, S. J. Brodsky, and H.-C. Pauli, Phys. Rev. D **41**, 3814 (1990).
[44] D. J. Gross, I. R. Klebanov, A. V. Matytsin, and A. V. Smilga, Nucl. Phys. B **461**, 109 (1996).
[45] A. Armoni, Y. Frishman, and J. Sonnenschein, Nucl. Phys. B **596**, 459 (2001).
[46] C. Hamer, Nucl. Phys. B **121**, 159 (1977).
[47] A. Retzker, J. I. Cirac, and B. Reznik, Phys. Rev. Lett. **94**, 050504 (2005).
[48] S. P. Jordan, K. S. M. Lee, and J. Preskill, Science **336**, 1130 (2012).
[49] S. P. Jordan, K. S. M. Lee, and J. Preskill, arXiv:1112.4833 [hep-th].
[50] D. Horn, Phys. Lett. B **100**, 149 (1981).
[51] P. Orland and D. Rohrlich, Nucl. Phys. B **338**, 647 (1990).
[52] S. Chandrasekharan and U.-J. Wiese, Nucl. Phys. B **492**, 455 (1997).
[53] R. Brower, S. Chandrasekharan, and U.-J. Wiese, Phys. Rev. D **60**, 094502 (1999).
[54] K. Kasamatsu, I. Ichinose, and T. Matsui, arXiv:1212.4952 [quant-ph].
[55] G. Szirmai, E. Szirmai, A. Zamora, and M. Lewenstein, Phys. Rev. A **84**, 011611 (2011).
[56] M. Mathur, J. Phys. Math. Gen. **38**, 10015 (2005).
[57] P. Orland, arXiv:1207.0455 [cond-mat.str-el].
[58] B. Doucot, L. B. Ioffe, and J. Vidal, Phys. Rev. B **69**, 214501 (2004).
[59] P. O. Fedichev, Y. Kagan, G. V. Shlyapnikov, and J. T. M. Walraven, Phys. Rev. Lett. **77**, 2913 (1996).
[60] J. L. Bohn and P. S. Julienne, Phys. Rev. A **56**, 1486 (1997).
[61] F. K. Fatemi, K. M. Jones, and P. D. Lett, Phys. Rev. Lett. **85**, 4462 (2000).
[62] P. Jordan, Z. Phys. **94**, 531 (1935).
[63] J. Schwinger, US Atomic Energy Commission Report NYO-3071, 1952 (unpublished).
[64] E. J. Mueller, Phys. Rev. A **70**, 041603 (2004).
[65] M. Mathur, Phys. Lett. B **640**, 292 (2006).
[66] M. Mathur, Nucl. Phys. B **779**, 32 (2007).
[67] R. Anishetty, M. Mathur, and I. Raychowdhury, J. Phys. A: Math. Th. **43**, 035403 (2010).
[68] B. Svetitsky and L. G. Yaffe, Nucl. Phys. B **210**, 423 (1982).
[69] B. Svetitsky, Phys. Rep. **132**, 1 (1986).
[70] G. 't Hooft, Nucl. Phys. B **138**, 1 (1978).
[71] S. Elitzur, R. B. Pearson, and J. Shigemitsu, Phys. Rev. D **19**, 3698 (1979).
[72] G. Bhanot and M. Creutz, Phys. Rev. D **21**, 2892 (1980).